Modeling High Altitude Electron Density Plumes Using Direct Numerical Simulation

Submitted to the Faculty of the

WORCESTER POLYTECHNIC INSTITUTE

Department of Physics

in partial fulfillment of the requirements for the

Degree of Master of Science

by

Autumn D. Paro

April 7, 2014

APPROVED:

Professor Alex Zozulya, Thesis Advisor

Dr. Jackie Schoendorf, Reader

Abstract

Electron densities form field-aligned structured regions in the natural ionosphere and after a high altitude nuclear explosion (HANE). These electron densities, known as plumes, are made up of many smaller individual field-aligned regions called striations. Striation modeling for systems effects has traditionally been done use a statistical approach. This statistical approach evolves different moments of the electron density. Due to lack of test data it has never been validated. The purpose of this project was to use a direct numerical simulation to solve equations governing the differential motion of individual striations. It was done in five steps: 1) Transport a single striation, 2) solve potential equation, 3) combine transport and potential equations, 4) optimize combined solver, and 4) simulate a fully-striated plume for comparison with the statistical model.

Acknowledgements

This work was performed from May 2012 to January 2014 under DTRA contract DTRA-01-03-0014 Task Order 0036 at Applied Research Associates. I would like to thank Jackie Schoendorf and Keith Siebert for mentoring on this project. I would also like to thank my Master's Thesis advisor, Professor Zozulya.

Contents

List of Figures

1 Introduction

Electron densities form field-aligned structured regions in the natural ionosphere and after a high altitude nuclear explosion (HANE). These electron density plumes stretch along magnetic field lines and instabilities can cause them to structure and break up into many smaller individual field-aligned striations (Figure 1.1). Small-scale striations pose problems because they can disrupt and degrade operation of communication and radar systems that are operating through them.

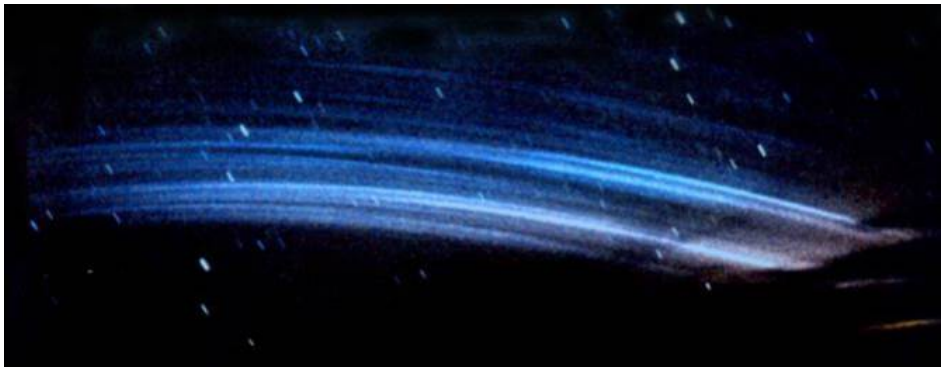

Figure 1.1: **Photo of field-aligned plasma striations 6 minutes after the Checkmate High Altitude Burst.**

Current models of high altitude nuclear environments use a statistical approach to account for striation structure because striation cross sections are much smaller than the practical lower limit on grid cell sizes. Striation Convection Theory (SCT) is the primary theory that underlies this statistical approach. It describes the collected motion of a fully-striated plume by evolving transport equations for different statistical moments of electron density. Due to the lack of relevant test data and limits on computational power needed to perform a large enough numerical simulation, SCT has never been validated. The goal of this project is to use Direct Numerical Simulation (DNS) to resolve individual striations and model their differential motion within a HANE-generated plume. This will be used to validate or invalidate SCT [1].

A direct numerical simulation (DNS) solves relevant computational fluid dynamics (CFD) equations by numerically resolving the solution in each cell of a computational mesh. Since SCT describes the collective motion of a fully-striated plume after structuring processes have stopped, equations in the DNS solution need to be tailored to inhibit structuring of individual striations. Eventually a large enough DNS will be performed to allow for simulation statistics to be compared to SCT, thereby validating or invalidating it.

1.1 Theory Behind Direct Numerical Simulation (DNS) of Field-Aligned Striations

Magnetic field-aligned striations have very little variation along the direction parallel to the magnetic field and therefore can be modeled as two-dimensional structures. The basis for striation modeling using DNS is two-dimensional magnetohydrodynamics. Motion of striations are characterized by an $\vec{E} \times \vec{B}$ drift where the striation velocity, $\vec{U}$, is computed as

$$\vec{U} = \frac{c}{|\vec{B}|^2}(\vec{E} \times \vec{B}) \tag{1.1}$$

where $\vec{B}$ is the background magnetic field and $\vec{E}$ is the electric field defined as the negative gradient of a potential, $\vec{E} = -\vec{\nabla}\phi$. The total density, N, evolves according to the continuity equation:

$$\frac{\partial N}{\partial t} + \vec{\nabla} \cdot N\vec{U} = 0, \tag{1.2}$$

where N is the sum of striation density, N_s, and background density, N_b. The two-dimensional potential used to calculated the electric field is a solution of the generalized Poisson equation

$$\vec{\nabla} \cdot N\vec{\nabla}\phi = \frac{1}{c}\vec{\nabla} \cdot N\vec{V_n} \times \vec{B} \tag{1.3}$$

where V_n is the neutral wind velocity and the only driving force in the problem [2][3][4][5].

1.2 OpenFOAM

OpenFOAM is an off the shelf open source software package used for numerical finite-volume CFD calculation. It consists of over 80 open source C++ libraries for partial differential equation, matrix inversion, and mesh generation, conversion, and manipulation. It also comes equipped with built in parallelization capabilities, its own pre- and post-processors, spatial and temporal discretization schemes, and an iterative method to invert linear systems. Due to the nature of open source software, the user can customize OpenFOAM solvers if they know the programming techniques used, physical principles behind their problem, and the underlying method used in OpenFOAM [6][7][8].

An OpenFOAM solver is made up of several parts: standard header files, user customized header files, equation solver, and time control. Figure 1.2 illustrates the flow of an OpenFOAM solver for the potential equation. OpenFOAM uses standard header files to error check, create the time variable, and build the mesh object. Other variables are defined and initialized in user customizable header files. During a solver run, OpenFOAM determines the variable time step using a Courant condition. During the time loop it solves the specified equations and recalculates the time step. At the final time step it exits the time loop and ends the code.

The user controls various parameters for each run from a set of input files. Input files are broken into three directories: *0, constant,* and *system*. The *0* directory contains initial conditions for the various fields including density, velocities, and other scalar or vector fields used in the simulation. The *constant* directory contains a file defining simulation constants and a sub-directory where mesh parameters, such as size and resolution, are defined. The *system* directory is where user defined time controls (*controlDict*), discretization schemes (*fvSchemes*), solver tolerances (*fvSolution*), density distributions (*setFieldsDict* or *funkySetFieldsDict*), and parallelization parameters (*decomposeParDict*) reside.

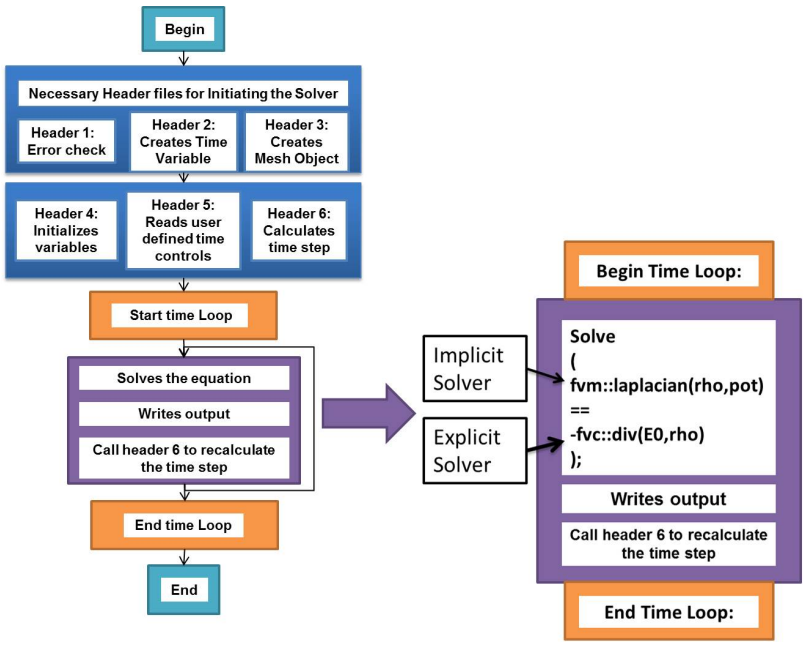

Figure 1.2: **Example of an OpenFOAM solver illustrating the flow of a solver and the direct interpretation of the potential equation.**

An OpenFOAM run requires the user to build the mesh using the OpenFOAM standard *blockMesh* utility. The density is distributed onto the mesh using either the *setFields* utility or the add on *funkySetFields* utility. The parallel processing utility *decomposePar* splits the mesh into segments that OpenFOAM places on multiple processors. During a solver run, OpenFOAM writes data for each time step into its own folder. For a parallel run each processor has its own set of time step folders and at the end of the run the user combines them using the *reconstructPar* utility. Run output can be viewed using a version of paraView that comes standard with OpenFOAM.

2 Methodology

The DNS of a fully-striated electron density plume was broken into several steps to allow for optimization and verification of the different equations and numerical schemes used to model them. The steps include:

1. Build an OpenFOAM solver that transports a single striation with minimal diffusion and deformation. Optimize transport equation for modeling multiple striations.

2. Solve the generalized Poisson equation for a single stationary striation. Optimize tolerance and number of iterations. Verify solution with analytic solution of a dielectric cylinder in a uniform electric field.

3. Combine transport and potential solvers with feedback between them. First solve potential equation, then use potential to solve for striation velocity, and transport striation using calculated velocity. Verify striation velocity using same techniques as potential solution.

4. Optimize solver for SCT scoping calculation. Increase mesh size to allow for multiple striations. Switch to a moving reference frame to keep striations from leaving the mesh without increasing compuational power. Run solver for two and four striations to test parallel processing and multiple striations. Include density initialization capabilities for randomly distributing striations of various densities and sizes‘ within a plume.

5. Perform an SCT scoping calculation of a fully-striated plume consisting of 100 randomly distributed identical striations. Perform initial comparison with SCT.

3 Results

3.1 Single Striation Transport

The OpenFOAM solver for single striation transport solves equation 1.2. This requires finding appropriate discretization schemes for time derivative and divergence operators. Without careful choice of discretization, the transported striation density may either diffuse (Figure 3.1A) or deform (Figure 3.1B). Diffusion is present in all hydrodynamic codes and can be reduced to an acceptable amount but cannot be removed entirely [9]. After comparing diffu-

sion from the nine OpenFOAM time derivative discretization schemes, the Crank Nicholson scheme was found to be the least diffusive. The CrankNicolson method is second order in time and is numerically stable [10].

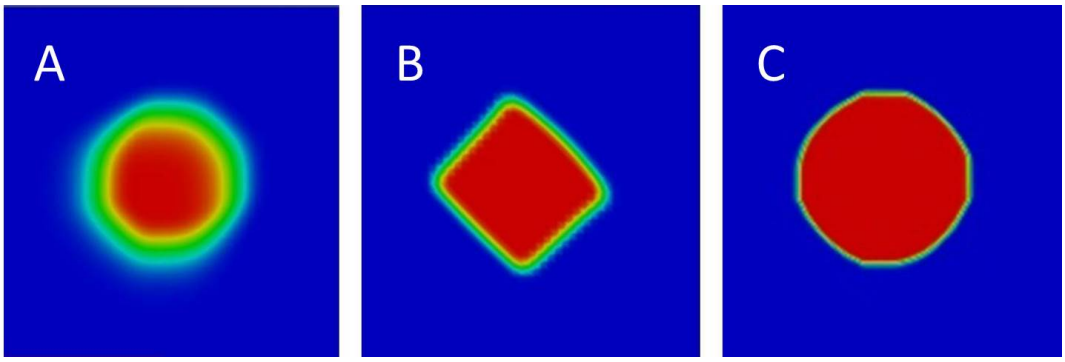

Figure 3.1: **After transport of the density of a circular striation, striation has: A) diffused, B) deformed, and C) transported accurately.**

OpenFOAM comes equipped with fifty different divergence schemes, some of which are significantly more diffusive than others. The least diffusive scheme, SuperBee, is a second order scheme that calculates exact peak value [11]. With SuperBee, the striation density transports without diffusion but deforms as it moves across the grid (Figure 3.1B).

We investigated several causes of the deformation, including whether the time derivative was solved implicitly or explicitly, and whether grid resolution was appropriate. Explicit time steps rely on the Courant condition which requires a limited time step to maintain numerical stability. Implicit schemes, on the other hand, are numerically stable but accuracy can be degraded if the time step becomes too large. For this problem both methods give the same deformed solution, but the implicit solver is faster. Tests of input parameters for the mesh and time step revealed that deformation was cause by too coarse of a grid and too large of a time step. By increasing the resolution and decreasing the time step parameters, the striation density was transported with minimal diffusion and deformation (Figure 3.1C).

3.2 Solve Generalized Poisson Equation

The potential equation (Equation 1.3) is solved for a single, stationary striation for optimization. Initial results show a different potential pattern for low density ratios, $\frac{N_s}{N_b} \leq 10$ (Figure 3.2A) and high density ratios, $\frac{N_s}{N_b} > 10$(Figure 3.2B). Tests determined that the different potential patterns were due to a lack of solver convergence at higher density ratios.

Numerical solvers have two criteria for solution control: tolerance and maximum number of iterations. Tolerance controls solution accuracy, which determines equality of two sides of an equation. For an iterative solver, such as that used in OpenFOAM, the calculation is repeated until the specified tolerance is reached. At high density ratios, the solver reached the default maximum number of iterations before obtaining the specified tolerance. Solver convergence and optimization requires finding the minimum tolerance and least number of iterations needed for an accurate solution over a range of density ratios. Results indicated that the minimum tolerance needed for large density ratios is 10^{-3}.

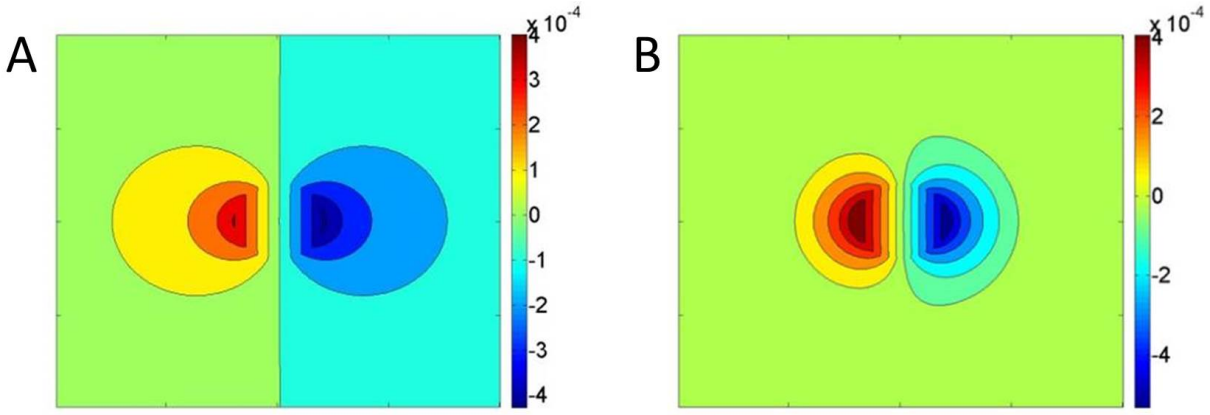

Figure 3.2: **(A) Correct potential pattern for low density ratios, $\frac{N_s}{N_b} \leq 10$, and (B)an incorrect potential pattern for high density ratios, $\frac{n_s}{n_b} > 10$. Initial conditions set the potential solution equal to zero at the boundaries.**

The numerical potential solution was verified by comparing it to the potential solution for a dielectric cylinder in a uniform electric field. The change in potential across the dielectric

cylinder is:

$$\Delta\phi_a = \frac{[\epsilon - 1]}{[\epsilon + 1]}\Delta\phi_0 \tag{3.1}$$

where $\epsilon = \frac{N_s}{N_b}$, $\Delta\phi_a$ is the potential drop across the cylinder, $\Delta\phi_0 = |\vec{E}|d_s$, d_s is the diameter of the cylinder, and $|\vec{E}|$ is the magnitude of the uniform electric field [12]. The numerical potential drop is calculated using $\Delta\phi_n = \phi_{max} - \phi_{min}$, which are the minimum and maximum potential values in the solution. To ensure the numerical solution is accurate, the potential solver was run for various density ratios and plotted against the analytic solution (Figure 3.3). The numerical solution matches the analytic solution for small density ratios and varies only slightly, by about 2%, for higher density ratios. The slight variation at higher density could be due to several factors including the low tolerance used in the solver.

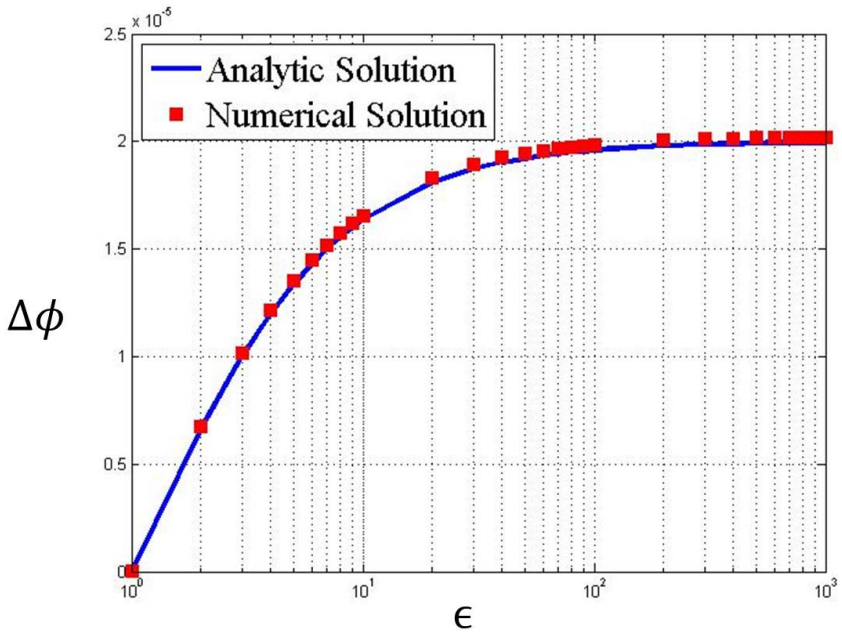

Figure 3.3: **Change in potential drop across a striation as a function of density ratio for both the numerical and analytical solutions.**

3.3 Combining Transport and Potential Solvers

The differential motion of a single striation is calculated using the transport and potential solvers with feedback between them. The new solver, combining these, first solves the generalized Poisson equation,

$$\vec{\nabla} \cdot N\vec{\nabla}\phi = \frac{1}{c}\vec{\nabla} \cdot N\vec{V}_n \times \vec{B}, \tag{3.2}$$

for the electric potential, ϕ. Using ϕ, it then calculates the striation velocity,

$$\vec{U} = \frac{c}{|\vec{B}|^2}(\vec{B} \times \vec{\nabla}\phi), \tag{3.3}$$

and transports the striation using $\vec{U}$,

$$\frac{\partial N}{\partial t} + \vec{\nabla} \cdot N\vec{U} = 0. \tag{3.4}$$

This solver was created for both a uniform and non-uniform density striation, since after a HANE it is not guaranteed that all striations will be of uniform density. Density for the non-uniform striations was calculated using $N = N_s e^{-r_s/d}$, where r_s is the striation radius and d is a constant (Figure 3.4).

The velocity for a uniform density striation was compared to the analytic solution for verification. Velocity is directly proportional to the potential drop across the striation:

$$\frac{\vec{U}}{\vec{V}_n} = \frac{\Delta\phi}{\Delta\phi_0} = \frac{[\epsilon - 1]}{[\epsilon + 1]}. \tag{3.5}$$

For initial conditions $\epsilon = 10$ and $\vec{V}_n = 1 \times 10^3 \frac{cm}{s}$, the analytic value is $\frac{9}{11} \approx 0.8182$. The numerical result is within 1.2% of the analytic value.

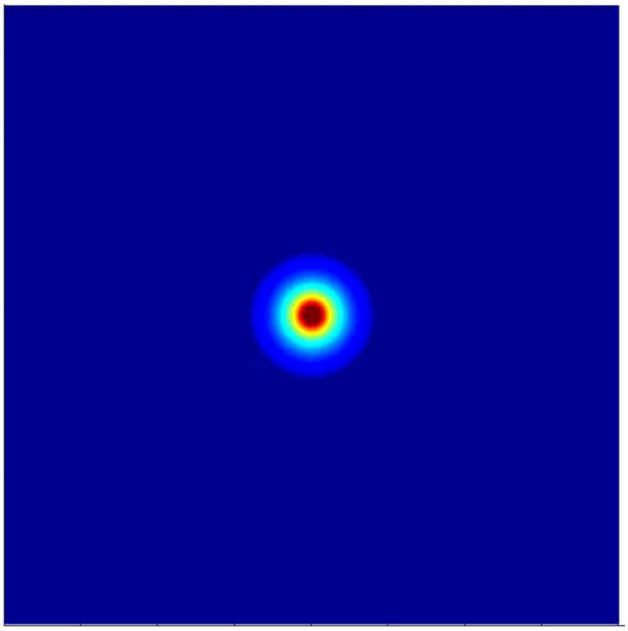

Figure 3.4: **Example of a non-uniform density striation.**

3.4 Optimizing Solver for Striation Convection Theory (SCT) Scoping Calculation

The combined solver will be used for SCT validation. This requires tens of thousand of striations of varying sizes and densities randomly distributed within the plume. To keep computation power low and allow for longer simulation times, the solver was converted to the moving reference frame. This prevents the striation from leaving the grid without increasing the grid size and computational power. To transform to the moving reference frame, the neutral wind velocity was subtracted from the striation velocity, making the new velocity equation

$$\vec{U} = \frac{c}{|\vec{B}|^2}(\vec{E} \times \vec{B}) - \vec{V}_n. \tag{3.6}$$

At low density ratios the striation will move in a downward direction because the striation velocity is slightly less than than the neutral wind velocity. As the density ratio increases, the striation velocity approaches the neutral wind velocity and the striation will move slower.

As simulation time is extended, striation structuring is evident (Figure 3.5). After a HANE, plumes structure and separate into smaller striations. These striations then structure and form even smaller striations. This process continues until a natural lower limit, called the freezing scale, is reached. There is no lower limit to striation size in the simplified DNS model therefore the structuring must be inhibited numerically. Plume structuring is driven by gradient drift instabilities that turn on when the downwind density gradient exceeds a certain threshold. Structuring observed in the simulation is consistent with this theory: uniform density striations (Figure 3.5) structure earlier than non-uniform density striations (Figure 3.6). Adding a diffusion term to the transport equation inhibits structuring by setting minimum striation size (Figure 3.7). The new transport equation is

$$\frac{\partial N}{\partial t} + \vec{\nabla} \cdot N\vec{U} - k\vec{\nabla}^2 N = 0 \tag{3.7}$$

where the magnitude of k, a constant, determines minimum striation size.

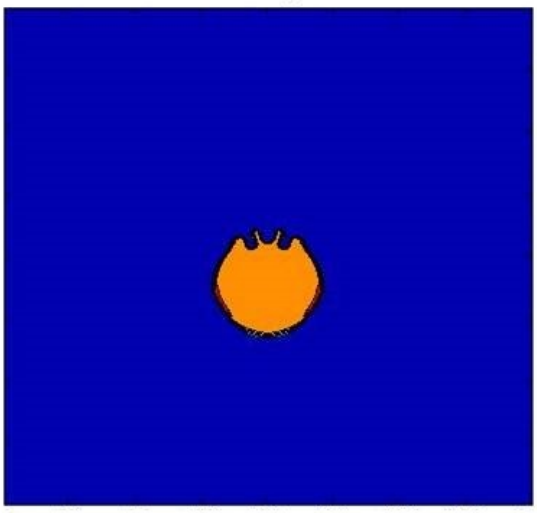

Figure 3.5: **Uniform density striation structuring and breaking up into smaller striations after 3s of simulation time in the moving reference frame with the neutral wind pointing in upwards direction.**

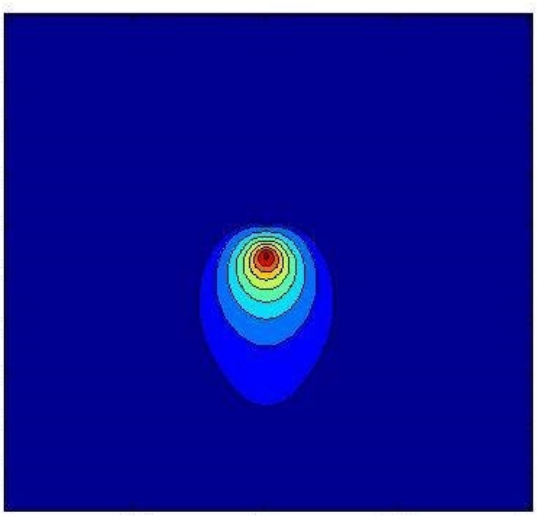

Figure 3.6: **Non-uniform density striation structuring after 9s of simulation time in the moving reference frame with the neutral wind pointing in upwards direction.**

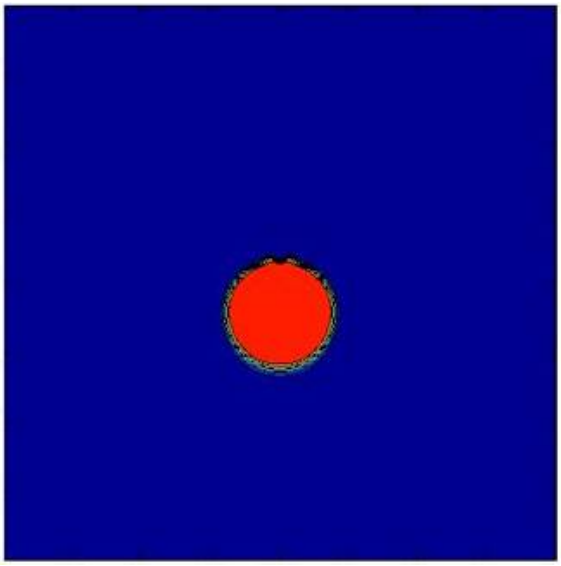

Figure 3.7: **Uniform density striation with structuring inhibited after 9s of simulation time in the moving reference frame with the neutral wind pointing in upwards direction.**

The mesh was initialized with both two and four striations to test parallel processing and interactions between striations in various orientations. For two striations the solver was tested with vertical (Figure 3.8) and horizontal orientations (Figure 3.10). After 10 seconds of simulation time, striations structure on the side facing the adjacent striation (Figures 3.9A and 3.11A). The lower striation in the vertical case structures more than the top striation. The associated potential pattern shows the two striations have distinct potential fields that are connected (Figure 3.9B). For the horizontal orientation, both striations structure on the downwind side of the inner edges. In this case, the potential field (Figure 3.11B) between the striations is stronger and the striations do not have distinct fields. Velocity contours are similar for both cases (Figures 3.9C and 3.11C).

The solver was tested for four striations in vertical, horizontal, diamond, and square orientations (Figure 3.12). Results for the diamond orientation show the striation densities elongate towards the center of the diamond and structure on the downwind edge (Figure 3.13A). Interactions between striations increases the value of the potential everywhere on the mesh (Figure 3.13B).

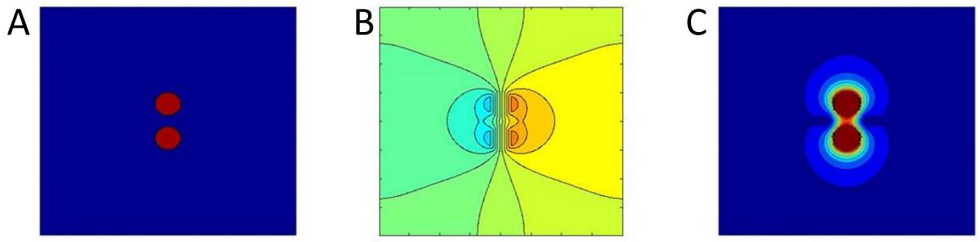

Figure 3.8: **A) Density, B) potential, and C) velocity, at t=0 s, for the vertical orientation of two striations in the moving reference frame with the neutral wind pointing in upwards direction.**

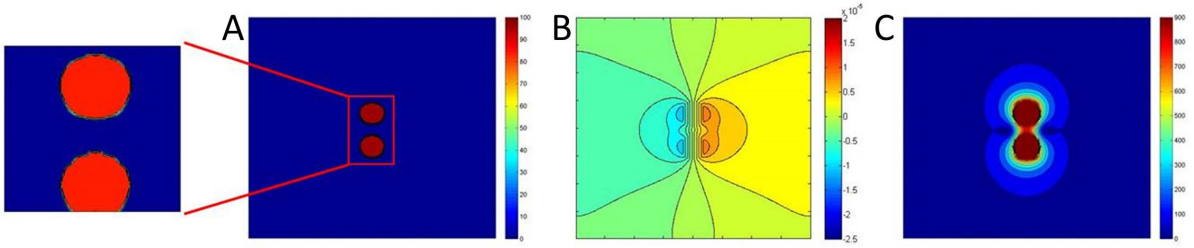

Figure 3.9: **A) Density, B) potential, and C) velocity, at t=10 s, for the vertical orientation of two striations in the moving reference frame with the neutral wind pointing in upwards direction.**

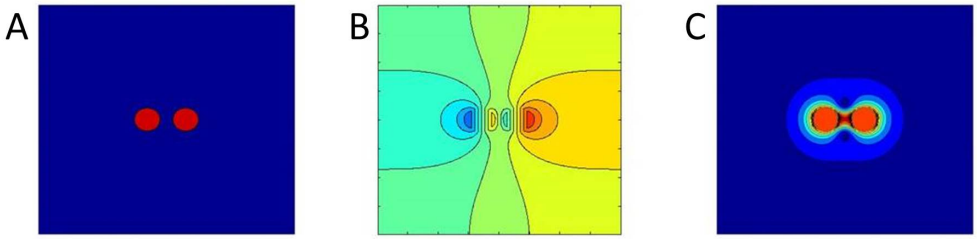

Figure 3.10: **A) Density, B) potential, and C) velocity, at t=0 s, for the horizontal orientation of two striations in the moving reference frame with the neutral wind pointing in upwards direction.**

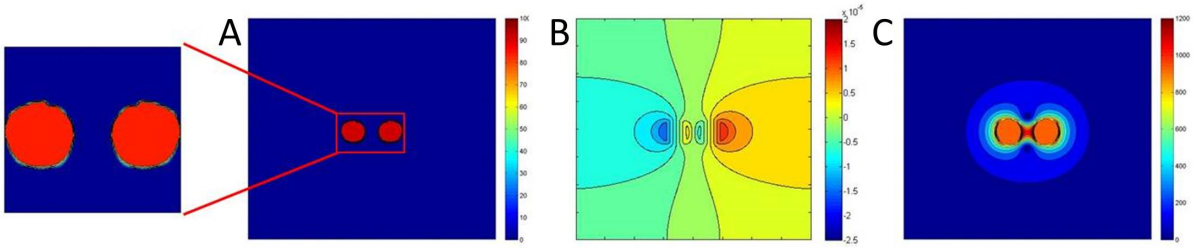

Figure 3.11: **A) Density, B) potential, and C) velocity, at t=10 s, for the horizontal orientation of two striations. This is in the moving reference frame with the neutral wind point in upwards direction.**

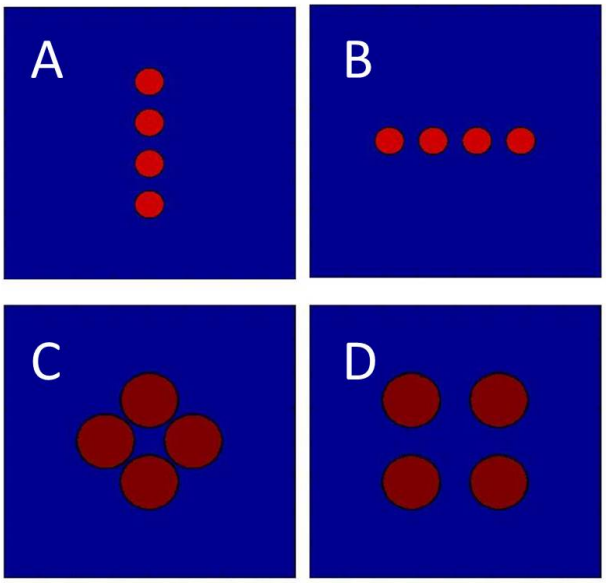

Figure 3.12: **Mesh initialized with four identical uniform density striations in four different orientations. These are in the moving reference frame with the neutral wind pointing in upwards direction.**

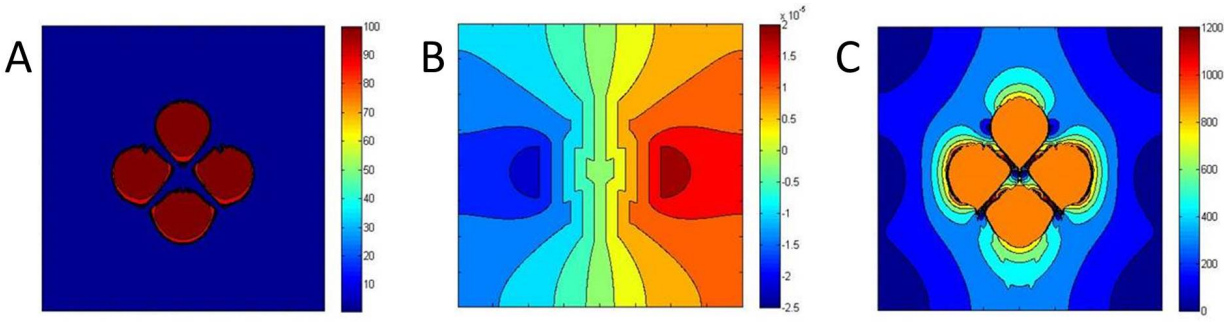

Figure 3.13: **A) Density, B) potential, and C) velocity, at t=10 s, for the diamond orientation of four striations in the moving reference frame with the neutral wind pointing in upwards direction.**

A fully-striated plume contains many striations of varying density randomly distributed in size and location. In order to initialize the OpenFOAM solver for a fully-striated plume, a separate C code was developed to randomize striation location and density based on user defined plume parameters including: number of striations, striation radius and density, uniform or non-uniform striation density, plume radius, and minimum striation separation. The code exports the striation data in a format read by the OpenFOAM add on *funkySetFields* which then distributes the density within the mesh. Multiple non-uniform density striation initialization requires the OpenFOAM extension *swak4Foam* for specification of density gradient equations within the field [13]. Using a probability density $P(a)$, where a is the characteristic radius, striation sizes are randomly distributed (Figure 3.16). These codes were created for both uniform (Figure 3.14) and non-uniform (Figure 3.15) striations.

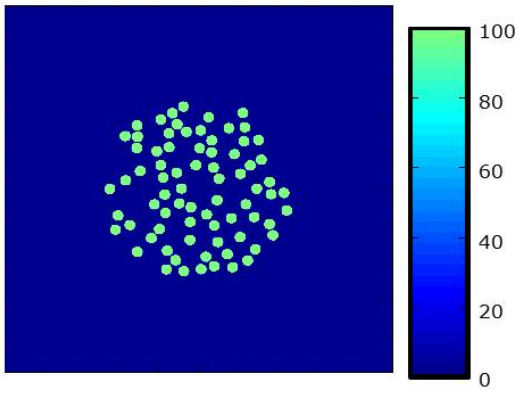

Figure 3.14: **Uniform density striations of uniform size randomly distributed within a plume.**

3.5 SCT Scoping Calculation

The SCT scoping calculation tests OpenFOAM's ability to model large scale simulations and evaluates computational costs needed for a full SCT validation simulation. It consists of 100 striations, radius 0.25 km, distributed within a plume of 5 km, with a density ratio of 100, in the moving reference frame (Figure 3.17). Simulation is performed on a grid of 20 x 20 km

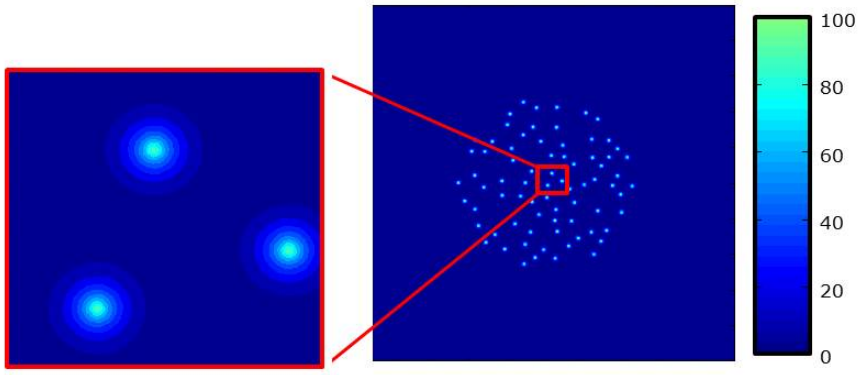

Figure 3.15: **Non-uniform density striations of uniform size randomly distributed within a plume.**

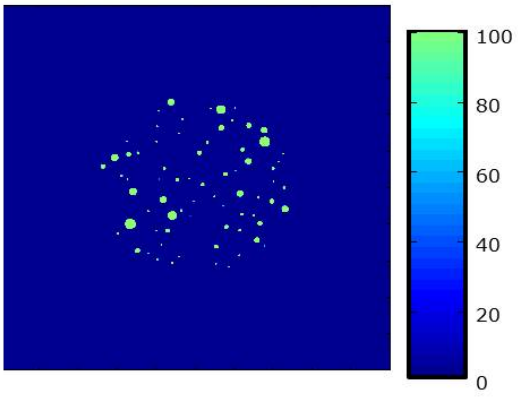

Figure 3.16: **Uniform density striations with sizes distributed according to $P(a) \approx \frac{1}{a}$, randomly distributed within a plume.**

with a cell size of 0.1 x 0.1 km giving a total of four million cells in the mesh. 30 seconds of simulation time took 20 hours real time, running on 16 processor cores on an IBM iDataPlex computer. The density profile (Figure 3.18A) shows striations structuring and breaking up into smaller striations even though a diffusion term was present (Equation 3.7). Striation structuring is seeded by the grid, and thus represents a source term not modeled by SCT. Therefore this run is not suitable for a full SCT test, however we can still use the early time results (before structuring) to perform important SCT validation tests.

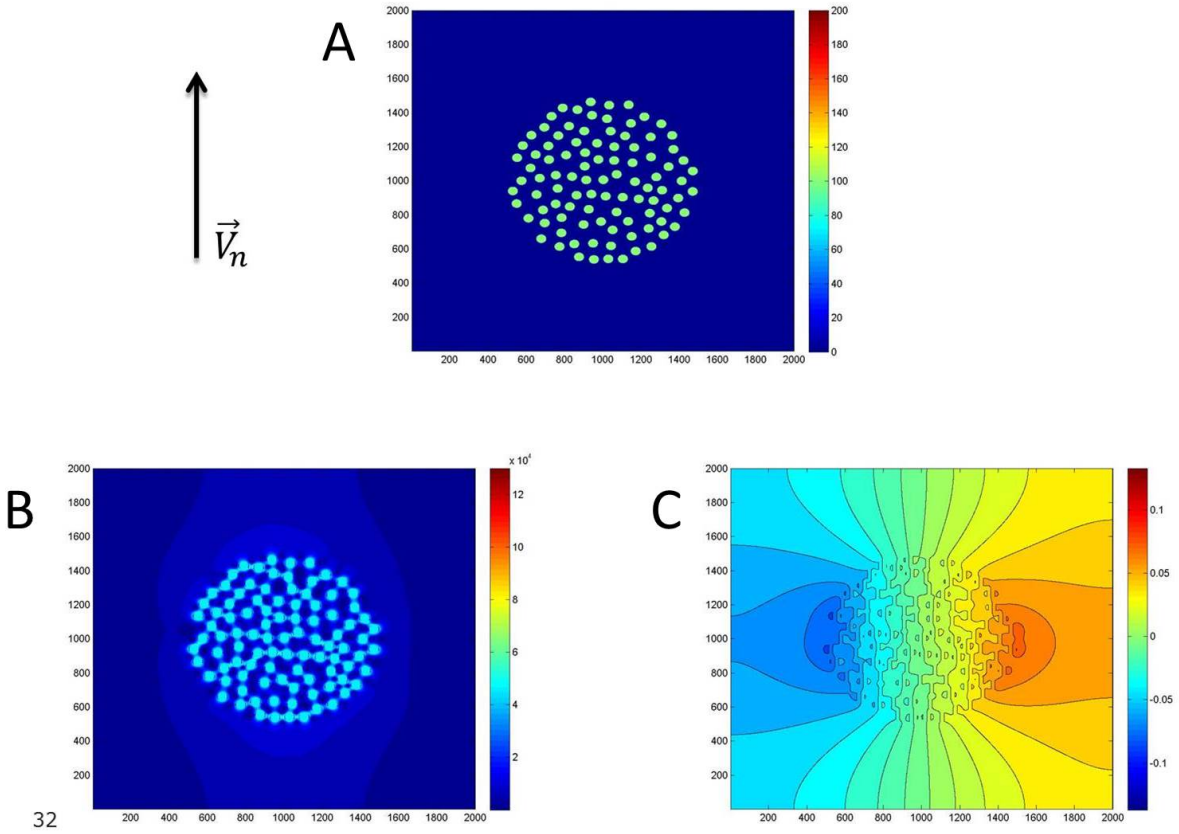

Figure 3.17: **SCT scoping calculation at t=0s for A) density, B) velocity, and C) potential in the moving reference frame.**

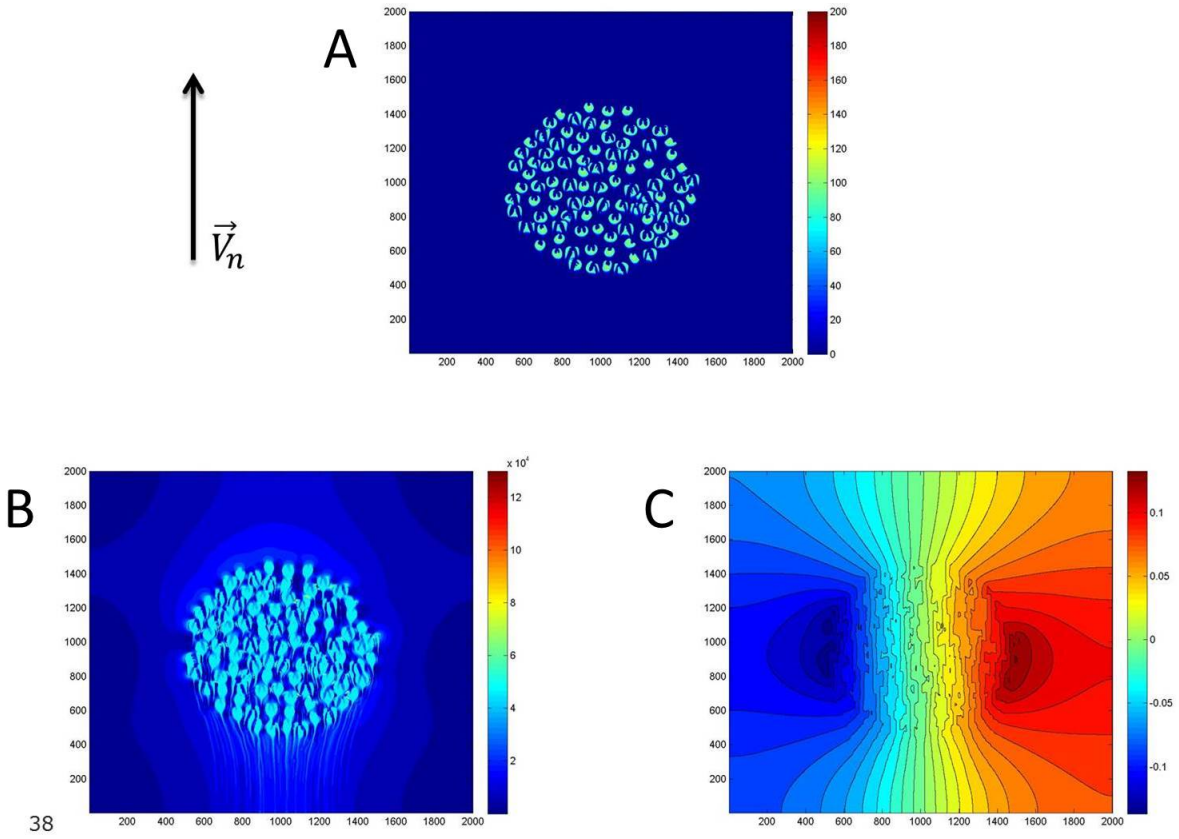

Figure 3.18: **SCT scoping calculation at t=30s for A) density, B) velocity, and C) potential in the moving reference frame.**

3.5.1 Striation Convection Theory (SCT)

SCT is a physical model of striated plasma evolution that evolves equations for different moments: $\langle N \rangle$, $\langle N^2 \rangle$, ..., $\langle N^m \rangle$. A choice of closure relation, where $\left\langle \frac{1}{N} \right\rangle$ is written in terms of $\langle N \rangle$ and $\langle N^2 \rangle$, is required to reduce the system to the first two moment equations. The flow velocity that convects average densities is computed from

$$\langle \vec{U} \rangle = \frac{c}{|\vec{B}|^2} (\vec{B} \times \vec{\nabla} \langle \phi \rangle), \tag{3.8}$$

where the average potential is substituted for the DNS potential. Equation for average potential depends on a smooth current approximation,

$$\left\langle \int dl \vec{J}_\perp \right\rangle = \int dl \vec{J}_\perp, \tag{3.9}$$

which means the field-line integral of the perpendicular current density does not vary on the striation scale. The smooth current approximation allows the electrostatic potential to be written as,

$$\vec{\nabla} \cdot \left\langle \frac{1}{N} \right\rangle^{-1} \vec{\nabla} \langle \phi \rangle = \frac{1}{c} \vec{\nabla} \cdot \left\langle \frac{1}{N} \right\rangle^{-1} (\vec{V}_n \times \vec{B}) \tag{3.10}$$

which is the same equation as for the unaveraged potential with N replaced with $\left\langle \frac{1}{N} \right\rangle^{-1}$. Thus even prior to the striation transport calculation, we can test the validity of the smooth current approximation with just the initial solution for electrostatic potential. We performed two tests: (1) whether the averaged potential is consistent with $\left\langle \frac{1}{N} \right\rangle^{-1}$ as SCT predicts or with $\langle N \rangle$ as might be predicted from simple analysis and (2) whether the modeled current density varies on the striation scale or is smooth across the plume.

3.5.2 Comparing DNS Results to SCT

Comparing DNS results to SCT requires the different averages to be computed from the DNS. The relevant averages are computed using

$$\langle N \rangle = \frac{1}{A} \sum N \Delta x \Delta y \tag{3.11}$$

$$\langle N^2 \rangle = \frac{1}{A} \sum N^2 \Delta x \Delta y \tag{3.12}$$

$$\left\langle \frac{1}{N} \right\rangle = \frac{1}{A} \sum \frac{1}{N} \Delta x \Delta y \tag{3.13}$$

$$\sigma^2 = \langle N^2 \rangle - \langle N \rangle^2 \tag{3.14}$$

$$\frac{\sigma}{\langle N \rangle} = \frac{\sqrt{\langle N^2 \rangle - \langle N \rangle^2}}{\langle N \rangle} \tag{3.15}$$

where A is the averaging area (area of the plume), N is the density in each cell, and $\Delta x \Delta y$ is the size of each cell. Computing the averages for the DNS simulation gives

$$\langle N \rangle = 25.0$$

$$\langle N^2 \rangle = 2400$$

$$\left\langle \frac{1}{N} \right\rangle = 0.74$$

$$\sigma^2 = 1775$$

$$\frac{\sigma}{\langle N \rangle} = 1.68.$$

Using the analytic solution mentioned in Section 3.3, the potential drop across a uniform density cylindrical column is given by

$$\frac{\Delta\phi}{\Delta\phi_{max}} = \frac{\epsilon - 1}{\epsilon + 1} \tag{3.16}$$

where ϵ is the density ratio, $\Delta\phi_{max} = \frac{V_n B}{c} d$, and d is the column diameter. Based on the averages from the DNS simulation, we can make two predictions for the average potential

drop across the striated plume. If the average potential drop is determined by $\left\langle \frac{1}{N} \right\rangle^{-1}$, as SCT predicts then we have

$$\epsilon = \frac{\left\langle \frac{1}{N} \right\rangle^{-1}}{N_b} = 1.316 \Rightarrow \Delta\phi_{plume} = (0.14)\Delta\phi_{max} = 0.07\, statvolts. \tag{3.17}$$

If the potential drop is determined by $\langle N \rangle$ then we have

$$\epsilon = \frac{\langle N \rangle}{N_b} = 25 \Rightarrow \Delta\phi_{plume} = (0.92)\Delta\phi_{max} = 0.46\, statvolts. \tag{3.18}$$

These are different by approximately a factor of seven. The potential drop calculated directly from the numerical solution (Figure 3.19) is approximately 0.16 statvolts, which is a factor of two higher than the analytic potential drop calculated from $\langle \frac{1}{N} \rangle^{-1}$. Figure 3.20 compares the DNS and SCT predictions over a range of density ratios. The DNS values are fit with a curve that corresponds to the previously derived solution of a dielectric cylinder in a uniform electric field (Equation 3.1) by adding a constant multiplicative factor, k, giving:

$$\Delta\phi_{DNS} = k\Delta\phi_{max}\frac{(\epsilon - 1)}{(\epsilon + 1)}. \tag{3.19}$$

Using $\left\langle \frac{1}{N} \right\rangle^{-1}$, SCT calculates the potential drop using

$$\Delta\phi_{SCT} = \frac{f_s\left(1 - \frac{1}{\epsilon}\right)}{2 + f_s\left(1 - \frac{1}{\epsilon}\right)}\Delta\phi_{max} \tag{3.20}$$

where $f_s = \frac{n_s * A_s}{A_p}$, n_s is the number of striations, A_s is the area of a single striation, and A_p is the area of the plume. This strongly points to an inadequacy of the smooth current approximation although further investigation is required.

The smooth current approximation implies a uniform current density over the spatial

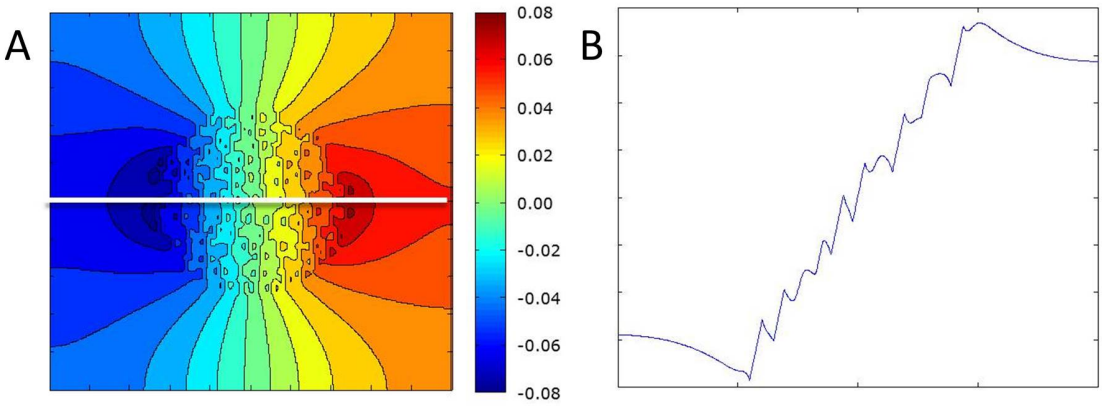

Figure 3.19: **A) Potential contour plot and B) Line plot of the potential through the center of the plume, for the SCT scoping calculation at t=0.1 s.**

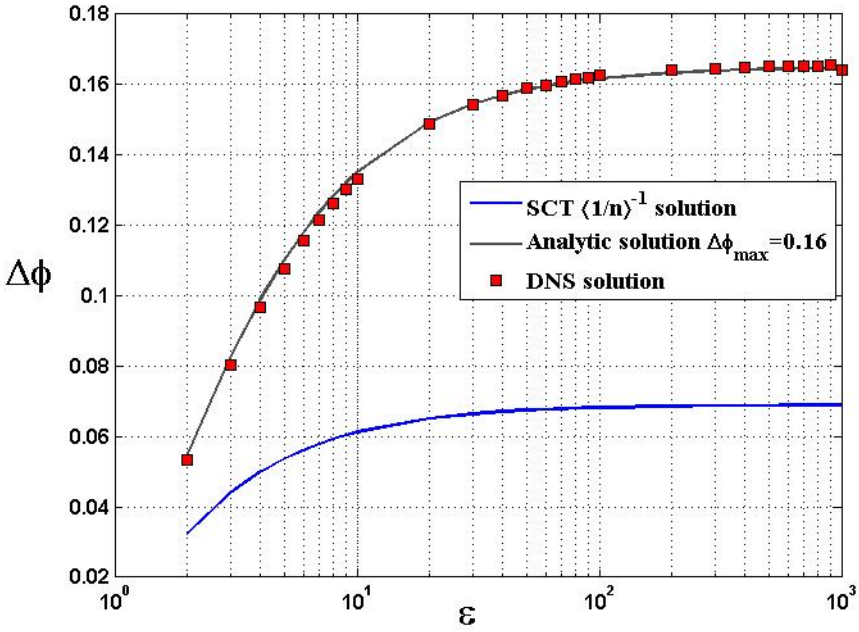

Figure 3.20: **Comparison of SCT predicted potential drop, analytical potential drop, and the DNS potential drop for different density ratios**

extent of the grid. To test the approximation, the current density equation,

$$J = N(-\vec{\nabla}\phi + \vec{V}_n \times \vec{B}), \tag{3.21}$$

was added to the existing OpenFOAM solver and the current density was plotted at t=0.1s, before structuring started. As the current density plot (Figure 3.21A) shows there is structuring on the striation scale but at a smaller magnitude than the striation density (Figure 3.21B). Further work is required to asses whether this result is evidence of the inadequacy of SCT.

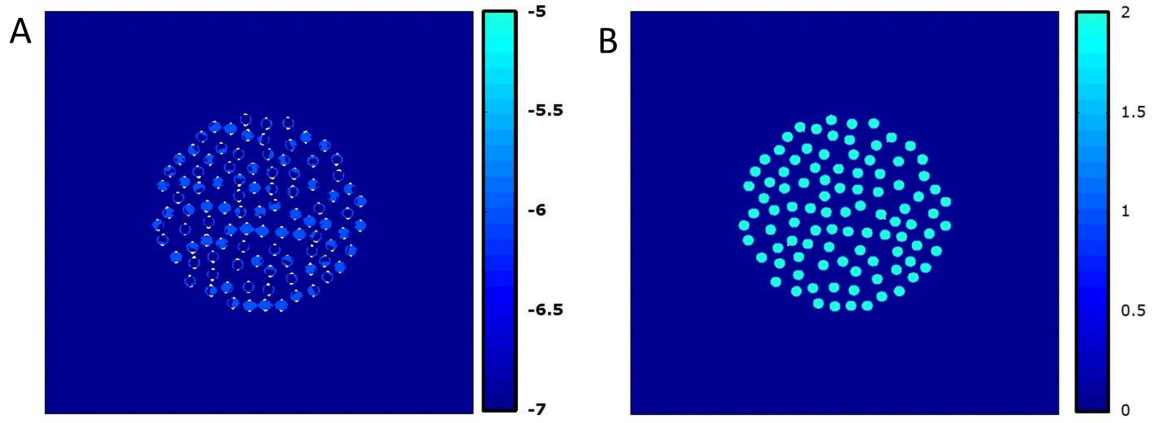

Figure 3.21: **Log plots of A) current density and B) striation density at t=0.1s.**

The final step is testing the closure relation. The closure relation is not unique to the problem and the SCT implementation in current HANE codes uses:

$$\left\langle \frac{1}{N} \right\rangle = \frac{\langle N^2 \rangle}{\langle N \rangle^3}. \tag{3.22}$$

Computing these averages for t=0.1 second gives

$$\left\langle \frac{1}{N} \right\rangle = 0.76 \left(\frac{1}{N_b} \right) \tag{3.23}$$

$$\frac{\langle N^2 \rangle}{\langle N \rangle^3} = 0.16 \left(\frac{1}{N_b} \right) \tag{3.24}$$

which are different by approximately a factor of five. This means that the closure relation is not valid for this case leading to the following questions. Is the restriction of the initial conditions imposed by the closure relation physically reasonable? If the closure relation is satisfied by the initial condition and then violated later on, then DNS does invalidate this particular implementation of SCT?

4 Conclusion

Electron densities form field-aligned structured regions in the natural ionosphere and after a high altitude nuclear explosion (HANE). These electron density plumes stretch along magnetic field lines and instabilities can cause them to structure and break up into many smaller individual field-aligned striations. Striation modeling for systems effects after a HANE has traditionally been done using Striation Convection Theory (SCT), a statistical approach that evolves different moments of the electron density. Due to lack of test data SCT has never been validated. The purpose of this project was to develop a direct numerical simulation that solves transport and potential equations governing the differential motion of individual striations with the ultimate goal of eventually using the DNS to validate or invalidate SCT. The DNS was developed in five steps: 1) transport a single striation, 2) solve potential equation, 3) combine transport and potential equations, 4) optimize combined solver, and 4) simulate a fully-striated plume for initial comparisons with SCT.

A Presentation Slides

WPI

Modeling High Altitude Electron Density Plumes Using Direct Numerical Simulation

Masters Thesis Defense
April 2014

Autumn Paro

Acknowledgements

- This work was performed under DTRA contract DTRA 01-03-0014 Task Order 0036 at Applied Research Associates
  - May 2012 – January 2014
- Thank you to Jackie Schoendorf and Keith Siebert for mentoring on this project
- Thank you to my Master's Thesis advisor, Professor Zozulya

Outline

- Background and Motivation
- Modeling differential motion of striations within an electron density plume
- Striation Convection Theory scoping calculation

Background

- Electron density forms field-aligned structured regions both in the natural ionosphere and after a high altitude nuclear burst
- After a burst, high density plumes of electron density stretch along magnetic field lines. Instabilities can cause the plumes to structure into many smaller individual field-aligned striations
- These small-scale striations can disrupt and degrade operation of communication and radar systems operating through them

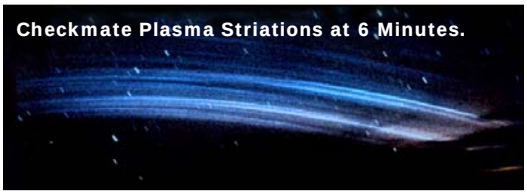

- A direct numerical simulation will be used to model motion of individual field aligned striations within a fully structured plume

Motivation

- Current high altitude nuclear effects (HANE) models use a statistical approach to account for structure because striation cross-sections are much smaller than model grid cells
- Primary theory that underlies the statistical approach is Striation Convection Theory (SCT)
  - Describes the collective motion of a fully-striated plume
  - Evolves transport equations for statistical moments of electron density
- SCT is used to model structure in HANE codes, but has never been validated
  - Lack of relevant test data
  - Until recently, it has not been possible to perform large enough numerical simulations to qualify as a validation test
- Goal of this project is to use Direct Numerical Simulation (DNS) to model the differential motion of electron density striations that occur after a nuclear burst
  - The DNS will be used to validate or invalidate SCT

5

Direct Numerical Simulation of Electron Density Striations

- A direct numerical simulation (DNS) solves relevant computational fluid dynamics (CFD) equations by numerically resolving the solution in each cell of computational mesh
- Since Striation Convection Theory (SCT) describes collective motion of a fully-striated plume, the DNS equations model the differential drift of individual striations
  - Equations are appropriate to model evolution of striations after structuring stops
  - Equations are not intended to represent processes that generate structure
- Eventually a large enough DNS will be performed so that statistics of the simulation can be compared to SCT

6

Steps for Modeling the Differential Drift of Individual Striations with DNS (1)

1) Transport an individual striation
   - Minimize diffusion and deformation of striation
2) Solve generalized Poisson equation for a stationary striation
   - Optimize solver tolerance and number of iterations
   - Verify solution with analytic solution of a dielectric cylinder in a uniform electric field
3) Combine transport and potential solvers with feedback between them
   - Solve potential equation, then solve velocity equation, finally use calculated velocity to transport striation
   - Verify striation velocity using same verification techniques as potential solver

Steps for Modeling the Differential Drift of Individual Striations with DNS (2)

4) Increase the size of mesh to allow for multiple striations
   - Requires switching to a moving reference frame so that striations do not reach the edge of the grid
5) Since a plume is made up of many striations, test equations and code with a few striations on the computational mesh
6) Conduct an SCT scoping calculation of a structured plume consisting of 100 randomly distributed striations
   - Perform initial comparisons against SCT

Equations for Striation Modeling with DNS

- 2-D electrostatic MHD is the basis for striation modelling with DNS
- Electron density, N, evolves according to transport equation:

$$\frac{\partial N}{\partial t} + \vec{\nabla} \cdot N\vec{U} = 0 \text{ where } \vec{U} = c\frac{\vec{E}\times\vec{B}}{B^2} \text{ and } \vec{E} = -\vec{\nabla}\phi$$

- 2-D electrostatic potential is solution to generalized Poisson equation:

$$\vec{\nabla} \cdot N\vec{\nabla}\phi = \frac{1}{c}\vec{\nabla} \cdot N\overrightarrow{V_n} \times \vec{B}, \text{ where } V_n \text{ is the neutral wind}$$

- This is a simplified version of the same model used to model Equatorial Spread F, the structures that occur in the natural ionosphere
- Solve these transport and potential equations using OpenFOAM

OpenFOAM Background

- OpenFOAM is off the shelf open source software used for numerical finite-volume CFD calculations
- Consists of over 80 open source C++ libraries
  - Partial differential equations
    - A variety of discretization schemes for the common operators

$$\vec{\nabla}^2, \vec{\nabla}\cdot, \vec{\nabla}\times, \vec{\nabla}, \frac{\partial}{\partial \mathrm{t}}, \frac{\partial^2}{\partial \mathrm{t}^2}$$

  - Matrix inversion
  - Meshing
    - Comes with its own mesh generator
    - Mesh parameters are specified by the user
    - A separate executable to generate the mesh
  - Post-processing
    - Includes a version of ParaView for visualization

OpenFOAM Solver

- OpenFOAM Solvers consist of:
  - OpenFOAM standard header files
    - Come from OpenFOAM shared libraries
  - User customized header files
    - All header files can be altered to suit the problem
    - In particular, Header 4 is user defined and specific to each solver
  - Equation solver
    - Direct interpretation of equation
    - Uses object oriented design
  - Time control
    - Reads in starting time, ending time, time step, and time step adjustability parameters
    - Calculates time step for adjustable time controls

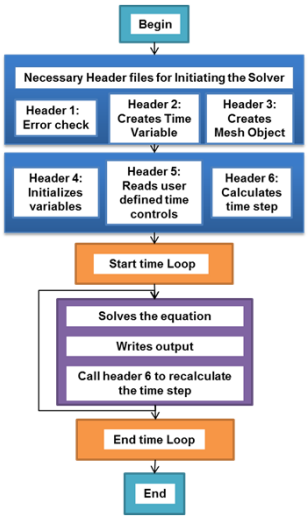

Transporting a Single Striation in All Directions (1)

- Investigated the various divergence schemes available in OpenFOAM
  - Certain schemes are less diffusive than others
  - Used the least diffusive divergence scheme, SuperBee
- Investigated solving the transport equation both implicitly and explicitly
  - Explicit schemes require limited time steps to maintain numerical stability
  - Implicit schemes are numerically stable but accuracy may be degraded if time step is too large
  - For our problem, implicit and explicit solver solutions were the same, but implicit solvers ran faster
  - The striation deformed regardless of which solver was used
- Tested the built in OpenFOAM anti-diffusion technique (MULES) and found that while it prevented diffusion, it also deformed the striation

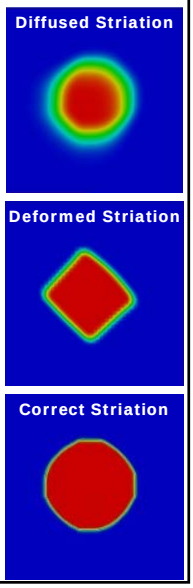

Transporting a Single Striation in All Directions (2)

- Investigation revealed that numerical deformation was caused by too large of a time step and too coarse of a grid
- Reduced time step by lowering time step parameters
- Determined appropriate resolution for an accurate solution
- Transports striation in all directions with minimal diffusion and deformation
- Algorithms were tested and verified for a single striation prior to introducing multiple striations

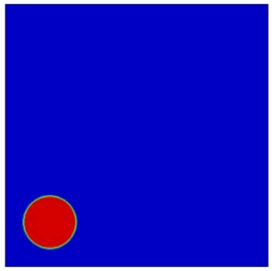

OpenFOAM Potential Solver

- Created a new solver that solved the simplified Poisson Equation

$$\vec{\nabla} \cdot \rho \vec{\nabla} \phi = -\vec{\nabla} \cdot \rho \vec{E}_0$$

  - $\rho = \rho_s + \rho_b$
    - ρ_s is the striation density
    - $\rho_b$is the background density
  - $\vec{E}_0 = -\frac{1}{c}(\vec{V}_n \times \vec{B})$
    - $\vec{V}_n$ is the neutral wind velocity
    - $\vec{B}$ is the uniform magnetic field
- Use input files to control values for $\rho_s, \rho_b, \vec{V}_n$, and $\vec{B}$

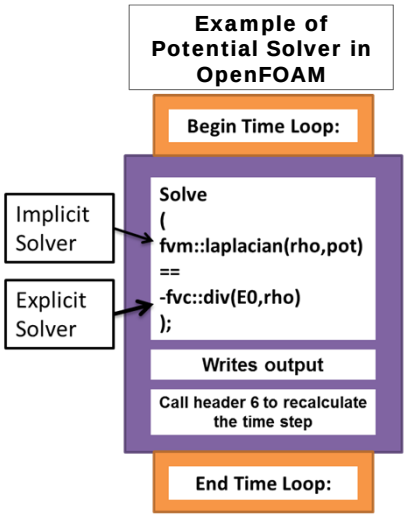

Potential Solver Convergence (1)

- Initial results showed a correct solution for small density ratios, $\frac{\rho_s}{\rho_b} \leq 10$, and an incorrect solution for larger density ratios, $\frac{\rho_s}{\rho_b} > 10$
  - Determined problem at large density ratios was due to lack of solver convergence

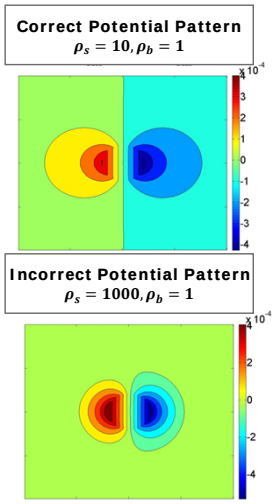

Potential Solver Convergence (2)

- The numerical solver has two criteria for how long it will run
  - Tolerance
    - How "equal" the two sides of the equation are
  - Number of iterations allowed (maxIter)
- At high density ratios the solver was reaching the maximum number of iterations before reaching the specified tolerance
- Performed an exercise to optimize the tolerance and number of iterations such that the solution converged
  - Exercise involved:
    - Upping maxIter so that it would never be reached
    - Changing the density ratio
    - Changing the tolerance
    - Determine lowest tolerance needed for an accurate solution by comparing solutions and numbers of iterations for different runs
    - Settled on a tolerance of 10^{-3}

Potential Solution Verification(1)

- Once the potential solution was obtained for larger density ratios the solution was verified against an analytic solution for a dielectric cylinder in a uniform electric field
- Compared the potential drop for the dielectric to the potential drop obtained in the simulation
  - The analytic potential drop was calculated using

$$\Delta\phi_a = \frac{[\epsilon - 1]}{[\epsilon + 1]}\Delta\phi_0$$

    - $\epsilon = \frac{\rho_s}{\rho_b}$
    - $\Delta\phi_a$ is the potential drop across the striation
    - $\Delta\phi_0 = |\vec{E}_0|d_s$
      - d_s is the diameter of the striation
  - The numerical potential drop was calculated from

$$\Delta\phi_n = \phi_{max} - \phi_{min}$$

Potential Solution Verification (2)

- Numerical calculations are in good agreement with the analytic potential drop for all density rations
  - Solutions identical for small density ratios
  - Numerical solution within 2% of analytic solution for large density ratios

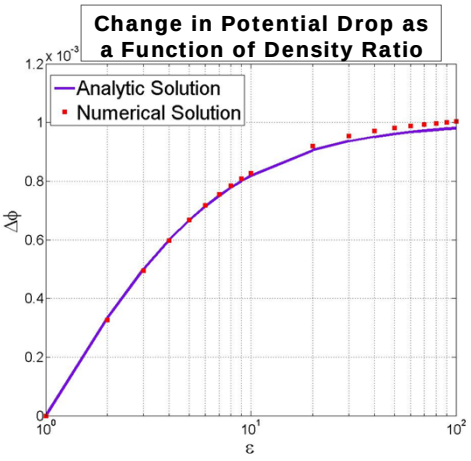

Combining Transport and Potential Equations

- Created a new solver that solves the potential and transport equations with feedback between the equations
- The new solver has three steps
  1. Solve the simplified Poisson equation
  2. Solve for the striation velocity using the calculated potential
  3. Solve the transport equation using the striation velocity
- This solver works with either uniform or non-uniform striation densities

Striation Velocity Verification

- To verify the numeric solution we again compared it to the analytic solution
- Since the velocity is directly proportional to the potential drop across the striation we used

$$\frac{\vec{U}}{\vec{V}_n} = \frac{\Delta\phi}{\Delta\phi_0} = \frac{[\epsilon - 1]}{[\epsilon + 1]}$$

  to verify our solution
- For our initial conditions we used:

  $\epsilon = 10, \vec{B} = 0.3\ \text{Gauss},\ R = 10\ \text{m},\ \text{and}\ \vec{V}_n = 1 \times 10^3\ \frac{\text{cm}}{\text{s}}$

  – The velocity ratio should evaluate to $\frac{9}{11} \approx 0.8182$

  – Numerical velocity was within 1.2% of analytic velocity

Ensure DNS Models SCT by Preventing Structure on Downwind Edge of Striations (1)

- After a HANE, plumes structure and separate into smaller striations as time progresses
  - These striations then structure and form still smaller striations
  - Process continues until natural lower limit for striation size is reached => this is referred to as the "freezing scale"
    - Observations suggest freezing scale ~1km
- SCT only models effects of differential motion of striations in a fully-structured plume after striations reach freezing scale
  - DNS should therefore prevent structuring of striations
- There is no lower limit to striation size in the simplified physical model we are using for DNS
- Therefore we need to inhibit structuring below the freezing scale in DNS simulations

Ensure DNS Models SCT by Preventing Structure on Downwind Edge of Striations (2)

- Striation structuring is driven by gradient-drift instabilities
  - Turns on when downwind density gradient exceeds threshold
- Structuring observed in simulations is consistent with theory
  - Uniform density striations structure much earlier than non-uniform density striations
    - Caused by a much steeper initial gradient
  - Larger striation to background density ratios inhibit structuring
- Adding diffusion term to transport equation inhibits structuring
  - Magnitude of coefficient sets minimum striation size

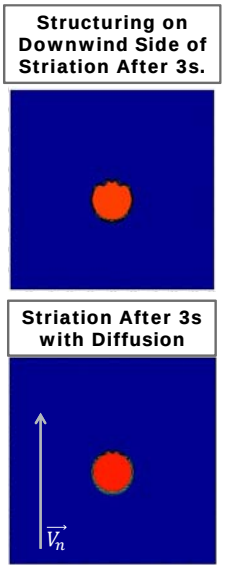

Preventing Striation from Leaving Mesh

- Transformed simulation to moving reference frame in order to prevent striation from leaving the mesh and allow for multiple striations
  - Neutral wind velocity was subtracted from the striation velocity
- At low density ratios, striation will move in downward direction
  - Striation velocity is slightly slower than neutral wind velocity

Striation Approaching Edge of Mesh at 3s

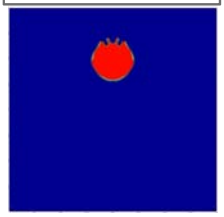

Striation After 3s in Moving Frame

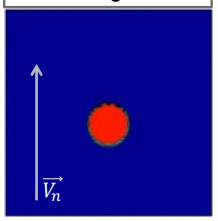

23

Modeling Multiple Striations (1)

- After a HANE, large numbers of striations are present
- SCT validation simulations must be initialized with several striations
  - Striations will have various cross-sections and densities
- Requires larger mesh, more computational power, and parallel processing
- Multiple striation modeling plan:
  - Start with two identical uniform-density striations
  - Increase number of striations for monitoring impacts on fields and computer resources
  - Randomly generate number of striations and each striation's position, cross-section, and density

Mesh Initialized with Multiple Striations of Various Sizes and Densities

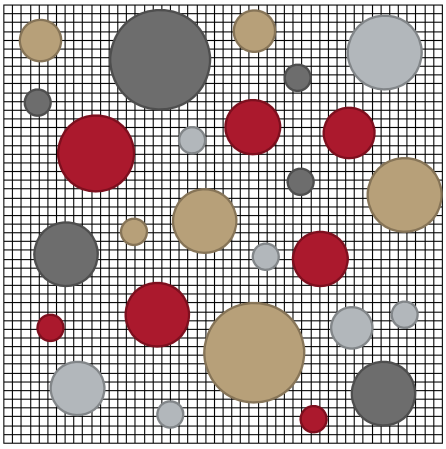

24

Modeling Multiple Striations (2)

- Initialize grid with two striations
  - Orientation of striations on grid impacts velocities and potentials
- Initialize grid with four striations
  - Test four possible orientations
  - Requires a larger mesh
  - Requires parallel processing

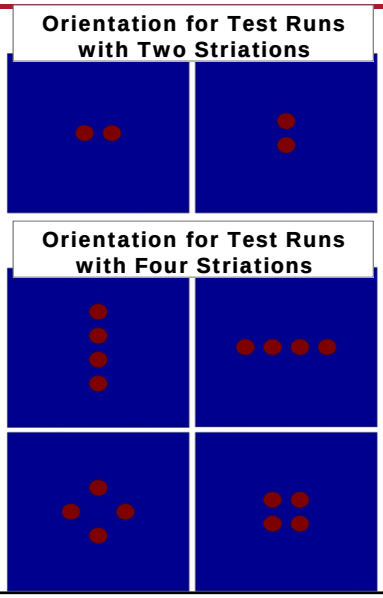

25

Modeling Multiple Striations (3)

- Vertical orientation in moving reference frame

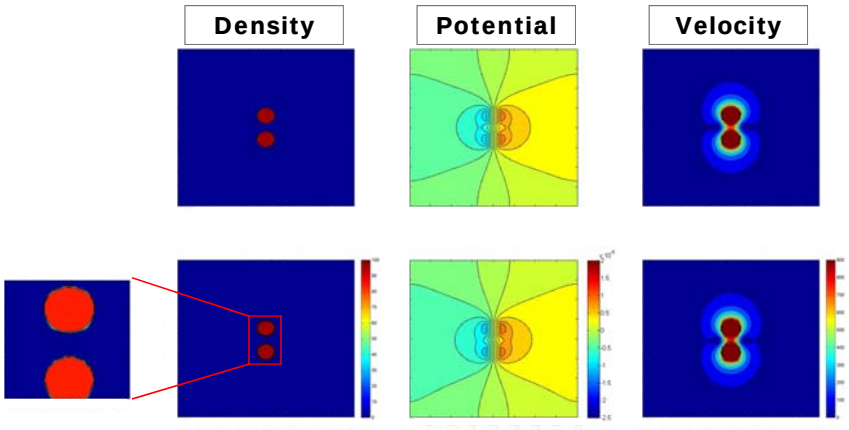

26

Modeling Multiple Striations (4)

- Horizontal orientation in moving reference frame

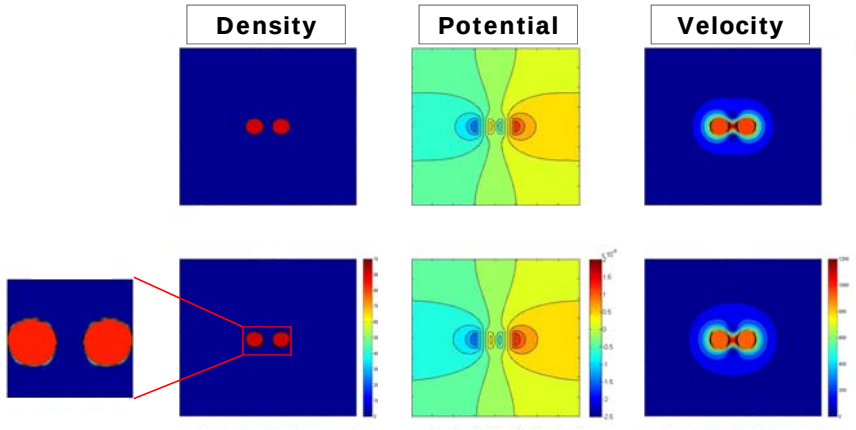

Modeling Multiple Striations (5)

- Four striations in moving reference frame

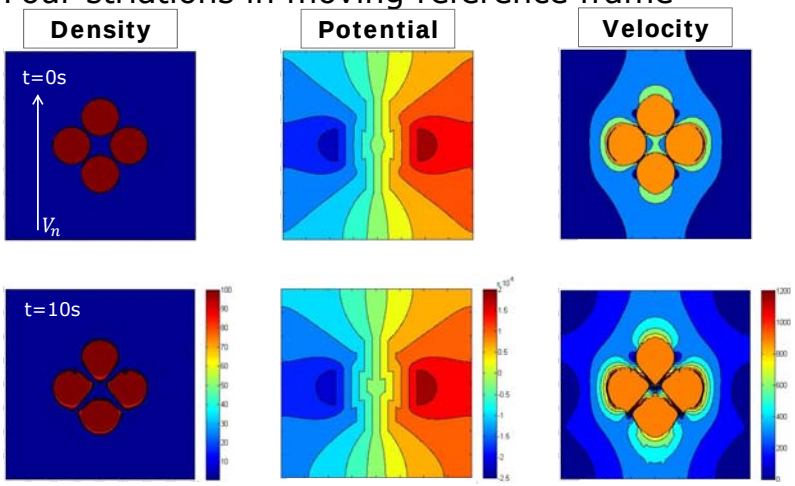

Initialization Capabilities to Model Striated Plume (1)

- After a HANE striations are randomly distributed in size and location within a plume
  - Striations have uniform or non-uniform density profiles
- Multiple uniform and non-uniform density striations
- Randomly distributed striation locations
  - Specify number of striations
  - Specify size of plume in which striations are distributed
- Random distribution of striation sizes based on specified probability distribution, $P(a)$ (where a is striation radius)
  - Allows user to control Power Spectral Density (PSD) of initial striation distribution
    - PSD related to and density profile of individual striations
  - Can be used for both uniform and non-uniform striation densities

Initialization Capabilities to Model Striated Plume (1)

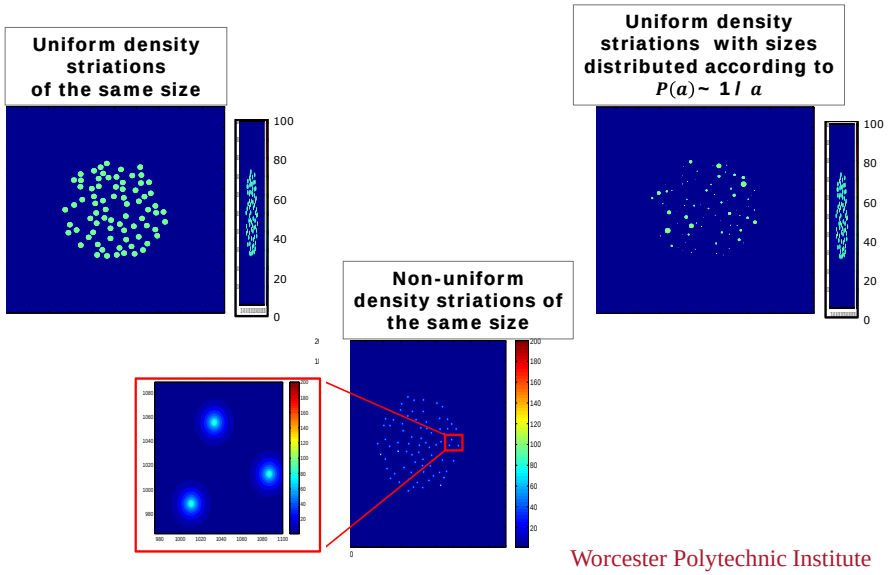

SCT Scoping Calculation

- A scoping calculation tests OpenFOAM's ability to model the large scale simulations necessary for SCT validation
  - Scoping calculation is a couple of orders of magnitude smaller than the full simulation, and consists of:
    - 100 Striations
    - Striation Radius: 0.25 km
    - Plume Radius: 5 km
    - Density Ratio: 100
    - Grid Extent: 20 x 20 km
    - Cell Size: 0.01 x 0.01 km
    - Number of cells: 4,000,000

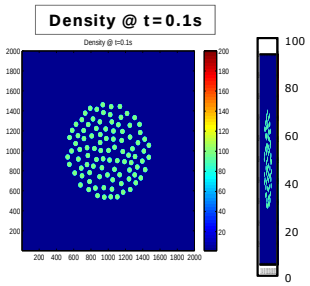

31

Worcester Polytechnic Institute

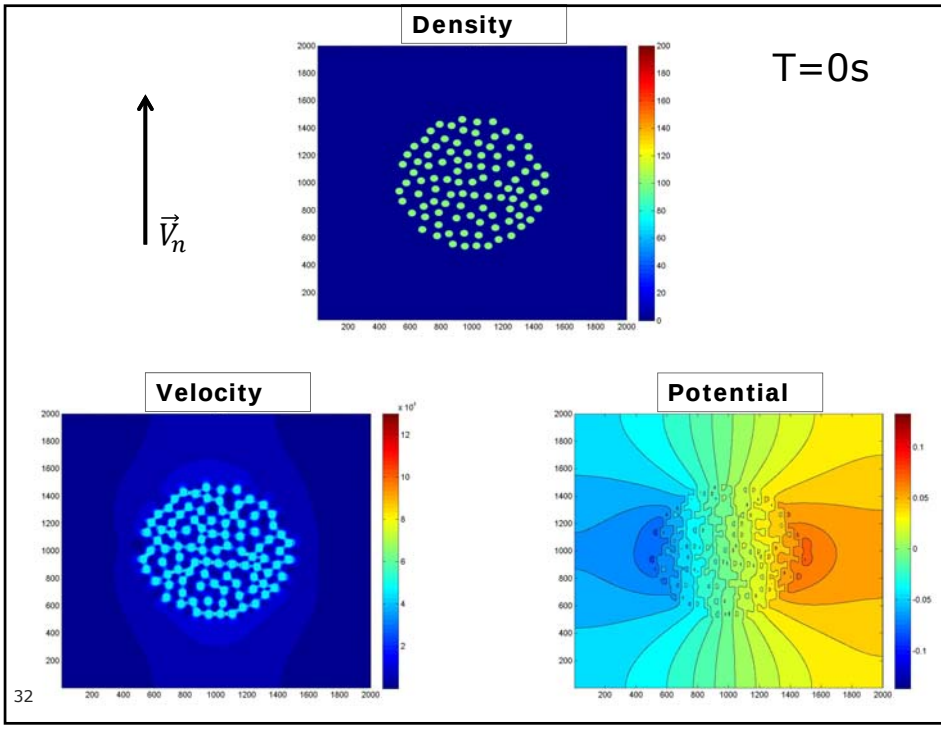

32

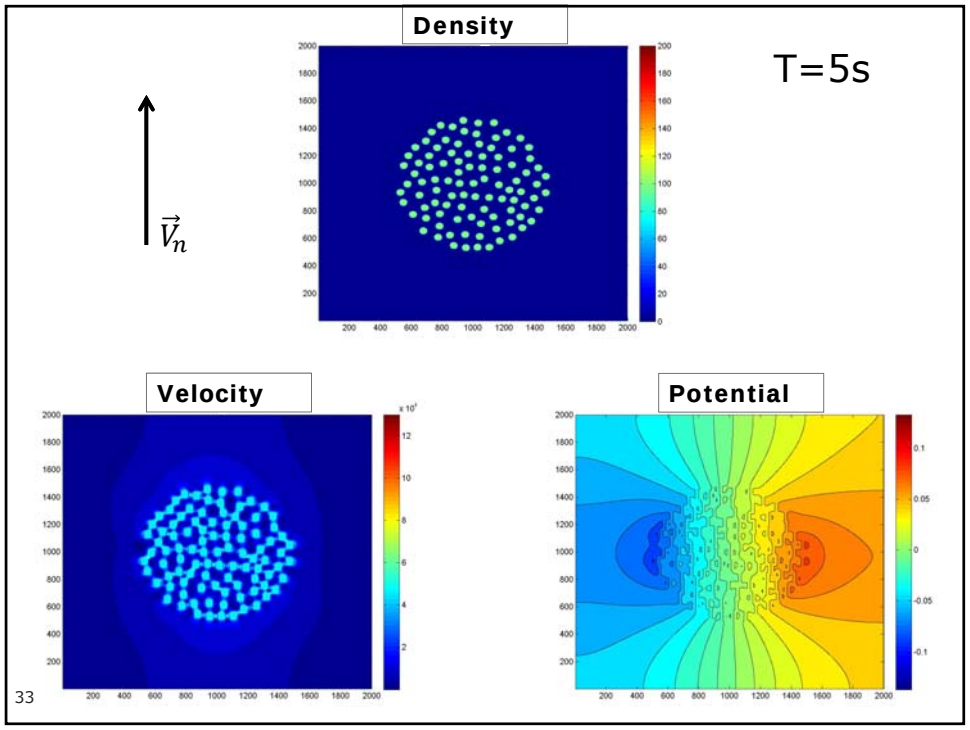
Density
T=5s
$\vec{V}_n$
Velocity
Potential

33

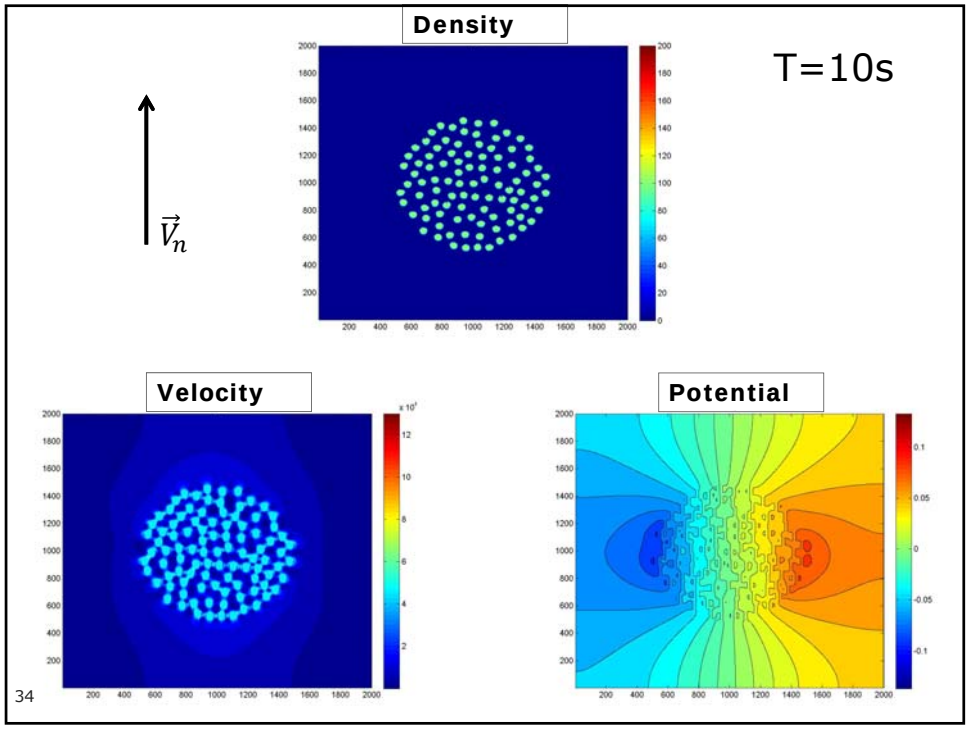
Density
T=10s
$\vec{V}_n$
Velocity
Potential

34

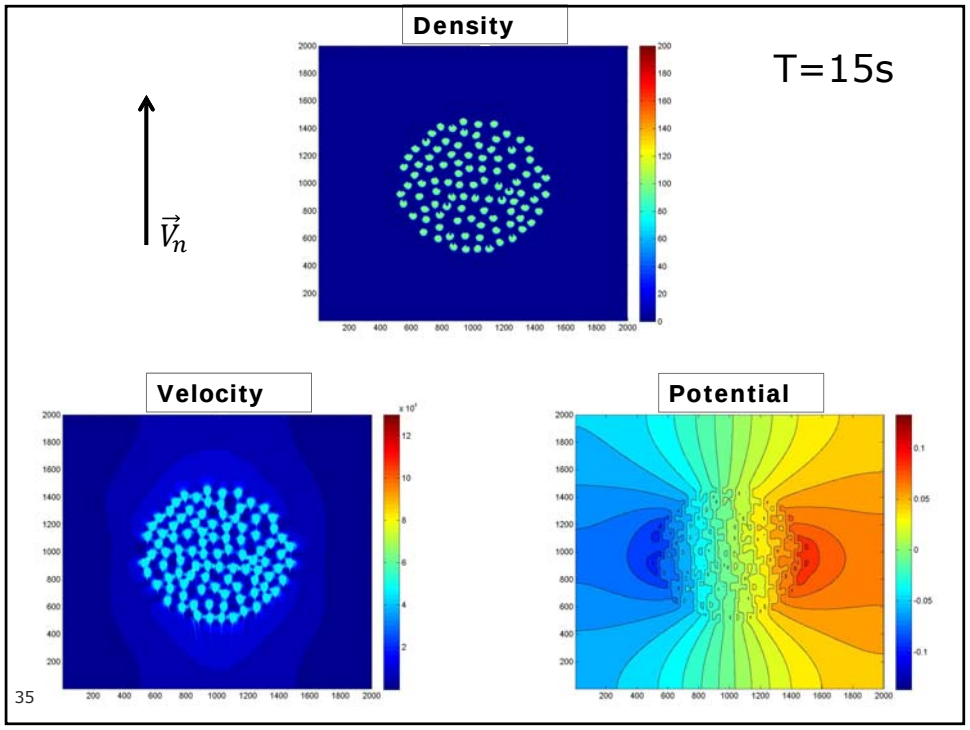
Density
T=15s
$\vec{V}_n$
Velocity
Potential
35

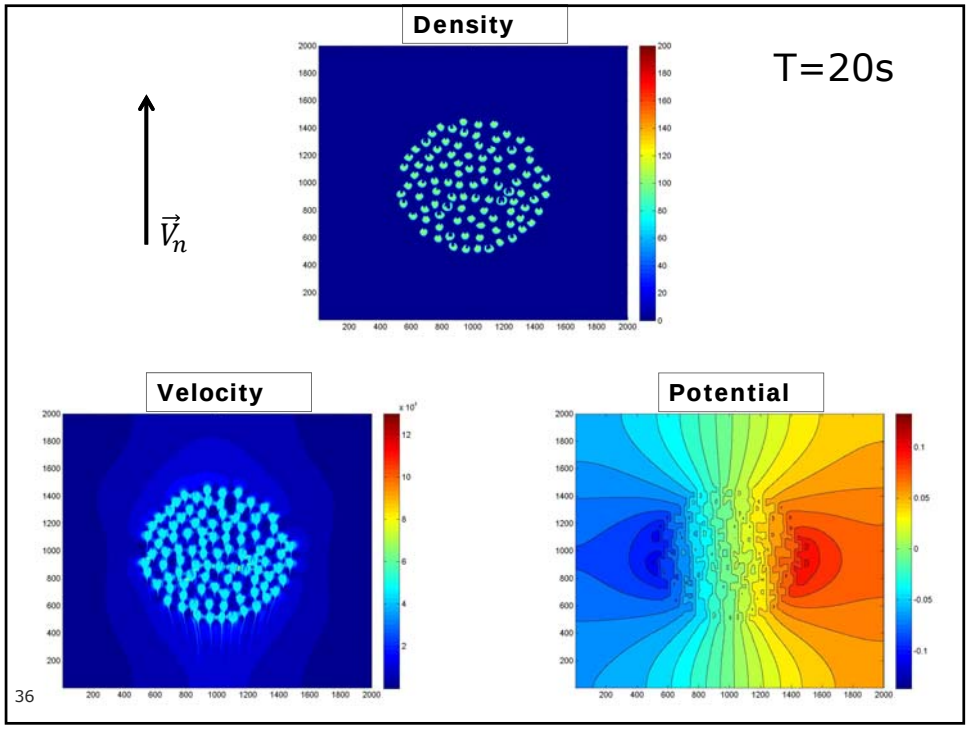
Density
T=20s
$\vec{V}_n$
Velocity
Potential
36

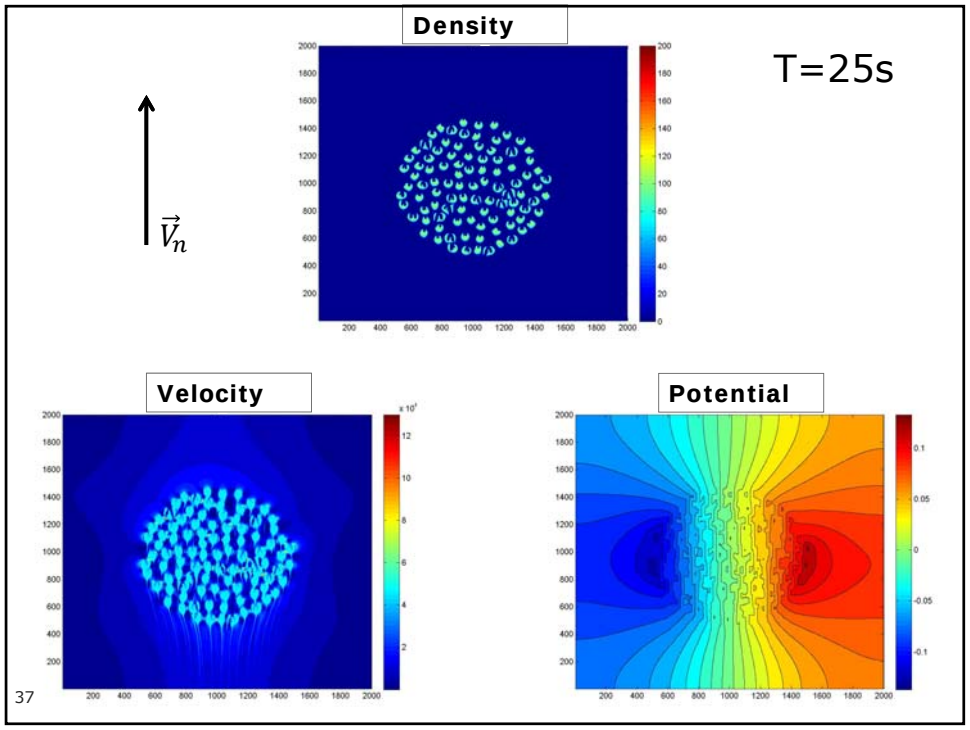
Density
T=25s
$\vec{V}_n$
Velocity
Potential
37

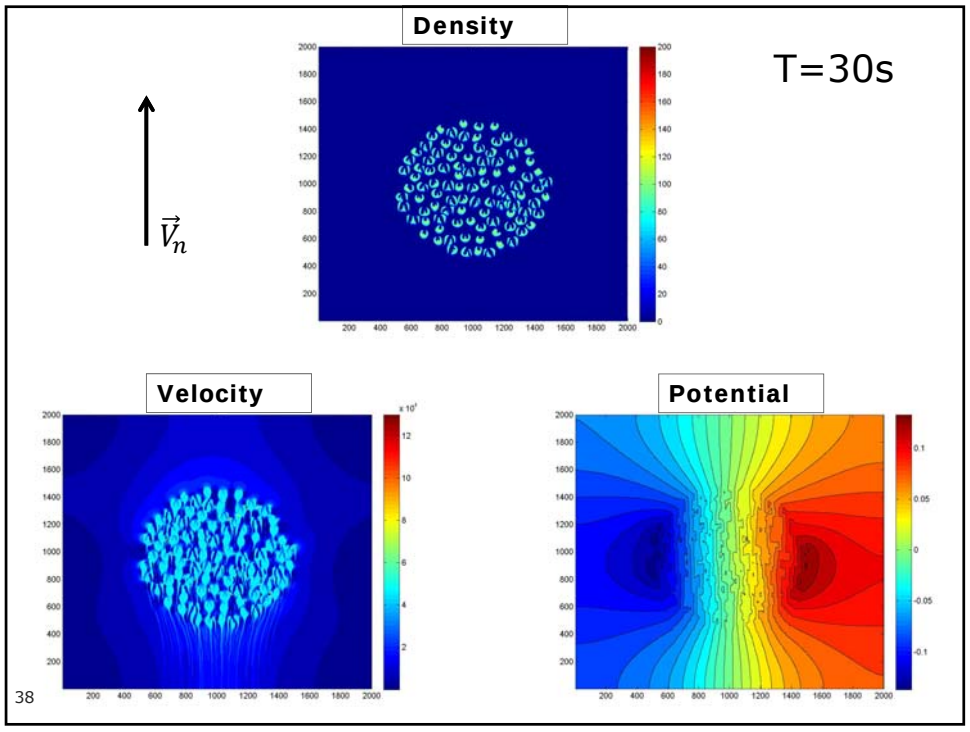
Density
T=30s
$\vec{V}_n$
Velocity
Potential
38

Scoping Calculation Analysis

- Computational statistics:
  - Simulation run on IBM iDataPlex (1092 compute nodes) at NAVO
  - 30s of simulation time took 20 hours running on 16 processor cores
- Simulation demonstrates capability, but not suitable for a full test of SCT because of striation structuring
  - Since structuring is seeded by the grid, it represents a source term that is not modeled by SCT
  - SCT models convection of fully striated plume after structuring mechanisms turn off
  - We have implemented a diffusion scheme to eliminate striation structuring, but it did not operate properly in this simulation
    - Under investigation
- However, there are still SCT validation tests we can perform on early-time simulation results (prior to structuring)

Striation Convection Theory (SCT) Background

- SCT is a physical model of striated plasma evolution
  - Evolution equations for $\langle N \rangle$, $\langle N^2 \rangle$,…, $\langle N^m \rangle$
    - $\langle \ldots \rangle$ is a spatial average over an area that contains a large number of striations
    - Reduction of system to the first two moment equations requires closure relation:
      - $\langle \frac{1}{N} \rangle$ in terms of $\langle N \rangle$ and $\langle N^2 \rangle$ (more on this later)
  - Flow velocity that convects averaged densities is computed from averaged potential:

$$\langle \vec{U} \rangle = c \frac{\vec{B} \times \vec{\nabla} \langle \phi \rangle}{B^2}$$

- Equation for averaged potential depends on assumption of "smooth current approximation"

$$\langle \int dl \, \vec{J}_\perp \rangle = \int dl \, \vec{J}_\perp$$

i.e. the field-line integral of perpendicular current density does not vary on the striation scale

DNS Diagnostics for Comparison with SCT

- Calculate the following averages using Matlab:
  - $\langle N \rangle = \frac{1}{A}\sum N\Delta x\Delta y$, Average density
  - $\langle N^2 \rangle = \frac{1}{A}\sum N^2\Delta x\Delta y$, Average squared density
  - $\langle \frac{1}{N} \rangle = \frac{1}{A}\sum \frac{1}{N}\Delta x\Delta y$, Average inverse density
  - $\sigma^2 = \langle N^2 \rangle - \langle N \rangle^2$, Square of density variance
  - $\frac{\sigma}{\langle N \rangle} = \frac{\sqrt{\langle N^2 \rangle - \langle N \rangle^2}}{\langle N \rangle}$
    - Where A is the averaging area, N is the density in each cell, and $\Delta x\Delta y$ is the size of each cell
- Calculate current density within OpenFOAM solver
  - $J = N(-\vec{\nabla}\phi + \vec{V_n} \times \vec{B})$

Diagnostics for Striated Plume

Statistics (applied over entire plume):

- $\langle N \rangle = 25.$
- $\langle N^2 \rangle = 2400$
- $\langle \frac{1}{N} \rangle = 0.74$
- $\sigma^2 = 1775$
- $\frac{\sigma}{\langle N \rangle} = 1.68$

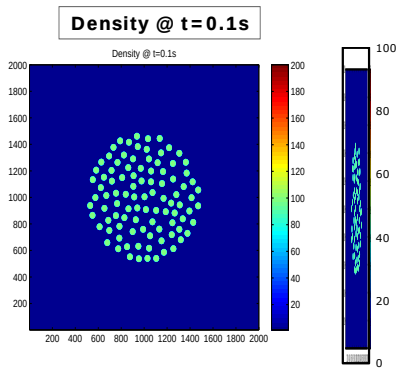

Averaged Potential Drop Across Striated Plume

- Potential drop across uniform density cylindrical column given by:

$$\frac{\Delta\phi}{\Delta\phi_{max}} = \frac{\epsilon-1}{\epsilon+1}$$

  - ϵ = ratio of column to background density
  - $\Delta\phi_{max} = \frac{V_n B}{c} d$, where d is column diameter

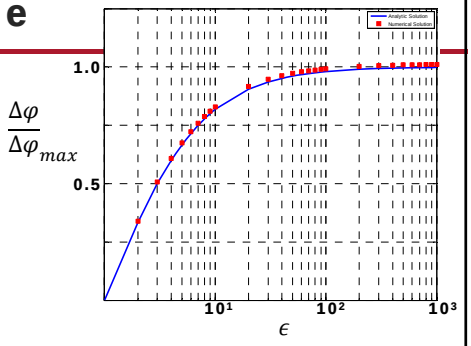

- If averaged potential in striated plume determined by $\langle\frac{1}{N}\rangle$, then:

$$\epsilon = \frac{\langle\frac{1}{N}\rangle^{-1}}{N_b} = 1.316 \Rightarrow \Delta\phi_{plume} = (0.14)\Delta\phi_{max} = 0.07 \text{ statvolts}$$

- If average potential in striated plume determined by $\langle N\rangle$ then:

$$\epsilon = \frac{\langle N\rangle}{N_b} = 25 \Rightarrow \Delta\phi_{plume} = (0.92)\Delta\phi_{max} = 0.46 \text{ statvolts}$$

43

Potential Drop Across Striated Plume

- SCT predicts potential drop of ≈0.07 statvolts
- DNS results show potential drop of ≈0.16 statvolts
- Possible sources of discrepancy
  - Inadequate statistics for determination of $\langle\frac{1}{N}\rangle^{-1}$
  - Inadequacy of smooth current approximation

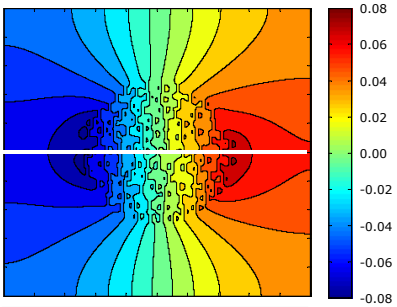

Potential Plot for SCT Scoping Calculation

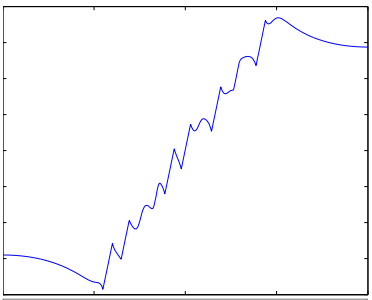

Potential Along Line Through Plume Center

44

Testing the Smooth Current Approximation (1)

- Smooth current approximation allows averaged electrostatic potential to be written as:

$$\vec{\nabla} \cdot \langle 1/N \rangle^{-1} \vec{\nabla} \langle \varphi \rangle = \frac{1}{c} \vec{\nabla} \cdot \langle 1/N \rangle^{-1} \vec{V}_n \times \vec{B}$$

- Note that this equation is the same as that for the unaveraged potential with N replaced by $\langle 1/N \rangle^{-1}$
- Thus even prior to full implementation of SCT equations, we can test validity of smooth current approximation with DNS of striated plume
  - Direct test: Are plots of $\vec{J}_\perp$ smooth over the spatial extent of plume?
  - Indirect test: Is averaged potential consistent with $\langle 1/N \rangle^{-1}$ rather than $\langle N \rangle$?

45

Worcester Polytechnic Institute

Testing the Smooth Current Approximation (2)

- Smooth current approximation implies no structuring in the current density, so we expect a constant value over the grid
- Current density shows structuring on the striation scale, but at a smaller magnitude
  - Further assessment of smooth-current approximation is required

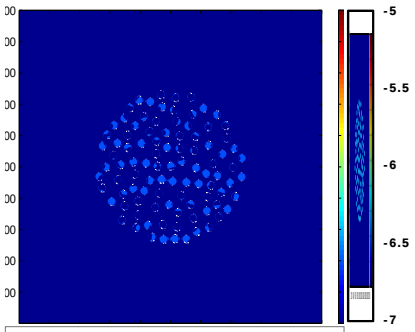

Log Plot of Current Density at t=0.1s

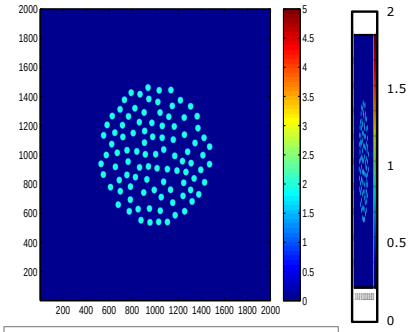

Log Plot of Density at t=0.1s

46

Comparing SCT Closure Relation and DNS Results

- Closure relation is not unique
- SCT implementation in HANE code uses:

$$\langle \frac{1}{N} \rangle = \frac{\langle N^2 \rangle}{\langle N \rangle^3}$$

- Computing these averages for the initial condition in 100 striation test case gives:
  - $\langle \frac{1}{N} \rangle = 0.76 \left(\frac{1}{N_b} \right)$
  - $\frac{\langle N^2 \rangle}{\langle N \rangle^3} = 0.16 \left(\frac{1}{N_b} \right)$
    - Different by factor ~ 5 ⇨ closure relation not valid for this case
- Two implications that require further study:
  - Is restriction of initial conditions imposed by closure relation physically reasonable?
  - If initial condition satisfies closure relation, then subsequent violation during DNS will invalidate this particular implementation of SCT

47

Results of Scoping Calculation

- Potential drop:
  - SCT predicts potential drop of ≈ 0.7 statvolts
  - DNS shows potential drop of ≈ 0.16 statvolts
  - Different by about a factor of ≈ 2
- Closure relation for initial conditions differ by a factor ≈ 5
- Test of smooth current approximation:
  - Current density structure exists on striation scale
  - Structure is approximately an order of magnitude smaller than initial condition

48

Summary

- Modeled motion of electron density striations in a neutral wind field and background magnetic field using Direct Numerical Simulation (DNS)
  - Solved generalized Poisson and transport equations using OpenFOAM
  - Conducted a scoping calculation of a structured plume with 100 randomly distributed striations for initial comparison with SCT

Questions?

References

[1] W. R. Wortman and R. W. Kilb. The relation between psds and striation properties. Final report dna001-77-c-0212, Mission Research Coporation, Santa Barbara, CA, 1978.

[2] S. T. Zalesak, P. K. Chaturvedi, S. L Ossakow, and J. S. Fedder. Finite temperature effects on the evolution of ionospheric barium clouds in the presence of a conductive background ionosphere l. the simples case: Incompressible background ionosphere, equipotential magnetic field lines, and an altitude-invarient neutra wind. *Journal for Geophysical Research*, 90:4299–4310, 1985.

[3] S. T. Zalesak, J. F. Drake, and J. D. Huba. Three-dimensional simulation study of ionospheric plasma clouds. *Geophysical Research Letters*, 17:1597–1600, 1990.

[4] F. W. Perking, N. J. Zabusky, and J. H. Doles III. Deformation and striation of plasma clouds in the ionosphere, l. *Journal of Geophysical Research*, 78.

[5] Michael C. Kelley. *The Earth's Ionosphere*. 1989.

[6] OpenFOAM Foundation. Openfoam, 2014 Available: http://www.openfoam.org.

[7] F. Raees, D. R. Van Der heul, and C. Vuik. Evaluation of the interface-capturing algorithm of openfoam for the simulation of incompressible immiscible two-phase flow, 2011.

[8] OpenFOAM Foundation. *OpenFOAM The Open Source CFD Toolbox User Guide*, 2.2.2 edition, September 2013.

[9] David H. Sowle and Thomas H. Johnson. Numerical methods of fluid dynamics, May 1975.

[10] J. W. Thomas. *Numerical Partial Differential Equations: Finite Difference Methods*. Springer-Verlag, 1 edition, 1995.

[11] Madhava Syamlal. Higher order discretization methods for the numerical simulation of fluidized beds. In *Fluidization anf Fluid-Particle Systems Topical Conference*.

[12] John David Jackson. *Classical Electrodynamics*. 3 edition, 1999.

[13] Openfoam wiki, 2013 Available: http://www.openfoamwiki.net/index.php/Contrib/swak4Foam.

[14] D. E. McDonald, S. L. Ossakow, and S. T. Zalesak. Scale sizes and lifetimes of f region plasma cloud striations as determined by the condition of marginal stability. *Journal of Geophysical Research*, 86:5775–5784, 1981.

[15] Tim Behrens. Openfoam's basic solver for linear systems of equations: Solvers, preconditioners, smoothers, 2009.

[16] Lehrstuhl fur Aerodynamik, Technische Universitat Munchen. *Anti-Diffusion method for interface steepening in two-phase incompressible flow*, 2009.

[17] Open Source CFD International Conference. *Computational continuum mechanics for sediment transport in free-surface flow*, 2008.